

Cite this: *Chem. Sci.*, 2023, **14**, 5266Received 29th January 2023  
Accepted 18th April 2023DOI: 10.1039/d3sc00487b  
[rsc.li/chemical-science](http://rsc.li/chemical-science)

## Design, synthesis, and application of some two-dimensional materials

Luwei Zhang,<sup>a</sup> Ning Wang \*<sup>a</sup> and Yuliang Li \*<sup>ab</sup>

Two-dimensional (2D) materials are widely used as key components in the fields of energy conversion and storage, optoelectronics, catalysis, biomedicine, etc. To meet the practical needs, molecular structure design and aggregation process optimization have been systematically carried out. The intrinsic correlation between preparation methods and the characteristic properties is investigated. This review summarizes the recent research achievements of 2D materials in the aspect of molecular structure modification, aggregation regulation, characteristic properties, and device applications. The design strategies to fabricate functional 2D materials starting from precursor molecules are introduced in detail referring to organic synthetic chemistry and self-assembly technology. It provides important research ideas for the design and synthesis of related materials.

### 1. Introduction

Creating and manipulating materials at the molecular or even atomic level has become an important development trend in chemistry and materials science.<sup>1–7</sup> Based on covalent or non-covalent bond interactions among the structural units with different functions, molecular material systems exhibit controllable physical and chemical functions.<sup>8–18</sup> The synthesis and assembly of molecular-based functional materials, the development of functional regulation, and related applications have become international research hotspots.<sup>19–22</sup> Especially, two-dimensional (2D) materials have gradually become one of the most attractive research directions.<sup>23–27</sup> When the functional segments are arranged in a 2D plane, some basic processes such as electron distribution and energy transport can only perform in the 2D-limited space, which would affect the intrinsic properties including mechanical properties, energy levels, conductivity, optical conduction, biochemical activity, etc.<sup>28</sup> Based on the above features, functional 2D materials have shown bright prospects in broad application fields including energy storage and transfer, catalysis, electric devices, biological medicines, etc.<sup>29–31</sup>

Until now, extensive research on functional 2D materials has been reported referring to a wide research field.<sup>32–36</sup> In the aspect of synthetic chemistry, new-emerging functional 2D materials have a significant feature that the building blocks are linked following the bottom-up preparation strategy starting

from the corresponding organic molecular precursors, which endows them with quite different fabrication processes, structural characteristics, and packing forms in contrast to the conventional materials.<sup>37</sup> Reported carbonic or organic 2D materials encompass the variable combination of structures and compositions because of the structural variety of organic precursors, and thus the structural feature can be systematically adjusted.<sup>38</sup> For instance, the size of the pores in the 2D planar framework can be adjusted by simply changing the chemical structure of precursors.<sup>39–42</sup> In addition, the linking way of the segments can be in different forms including covalent bonds, such as carbon–carbon bonds and carbon–heteroatom bonds; noncovalent interactions, such as hydrogen bonds, metal coordination bonds, and host–guest interactions, which efficiently expand the available reaction that can be used to prepare 2D materials.<sup>43–52</sup> On the other hand, a variety of packing forms and aggregation morphologies such as nanosheets, nanowires, and even multiscale nanostructures can be controllably formed.<sup>53</sup> On this basis, the facile introduction of metal atoms or other types of hybrid components can further expand their component and performance.<sup>54</sup> As a result, synthetic 2D materials are capable of exhibiting controlled physical properties in a broad range: the mechanical properties including mechanical strength, flexibility, and stretch ability can be efficiently tuned;<sup>55,56</sup> the electronic band structures can be designed as direct or indirect semiconductors;<sup>57</sup> the conducting properties can be adjusted in a wide range including metallicity, semimetals, insulators, and semiconductors;<sup>58,59</sup> the light-harvesting ability can range from the ultraviolet to infrared region.<sup>60,61</sup> The above advantages make functional 2D materials show great development potential in the corresponding application field (Fig. 1).

<sup>a</sup>Shandong Provincial Key Laboratory for Science of Material Creation and Energy Conversion, Science Center for Material Creation and Energy Conversion, School of Chemistry and Chemical Engineering, Shandong University, 27 Shanda Nanlu, Jinan 250100, P. R. China. E-mail: [wang\\_ning@sdu.edu.cn](mailto:wang_ning@sdu.edu.cn); [ylli@iccas.ac.cn](mailto:ylli@iccas.ac.cn)

<sup>b</sup>Key Laboratory of Organic Solids, Institute of Chemistry, Chinese Academy of Sciences, Zhongguancun North First Street 2, Beijing 100190, P. R. China



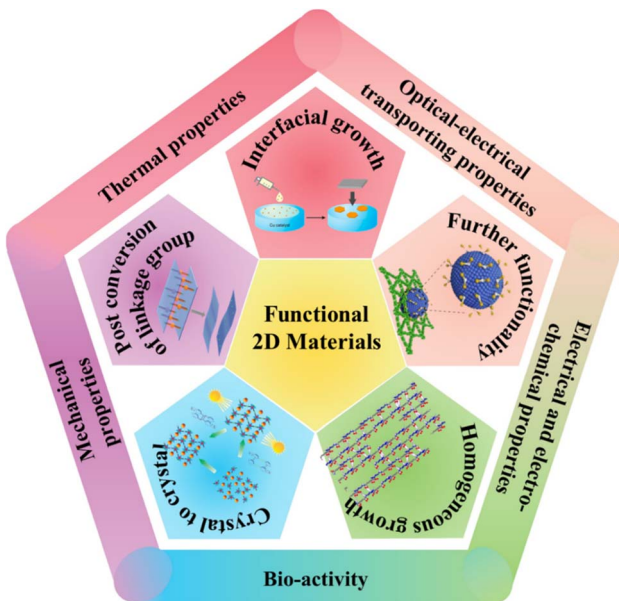


Fig. 1 Schematic illustration for the contents. Image for crystal-to-crystal: adapted from ref. 62. Copyright 2021, American Chemical Society. Image for homogeneous growth: adapted from ref. 63. Copyright 2022, Springer Nature. Image for interfacial growth: adapted from ref. 64. Copyright 2017, American Chemical Society. Image for post-conversion of the linkage group: adapted from ref. 65. Copyright 2018, John Wiley & Sons. Image for further functionality: adapted from ref. 66. Copyright 2022, American Chemical Society.

Functional 2D materials have developed into a huge material system that perfectly combines the structural features of traditional 2D materials, the electronic properties of conjugated functional materials, the structural variety of organic molecules, and manipulation advantage of supramolecular assembly, which have shown implications for a wide scientific community.<sup>67–69</sup> Although extensive review articles have emerged to introduce the recent advancement of 2D materials, to the best of our knowledge, only an individual aspect is focused, such as the particular kind of structure or certain type of the device application.<sup>70–74</sup> At the current stage, the ordered growth of the precursor in the 2D direction is one of the key scientific problems in the construction of synthetic 2D materials. Efficiently fabricating organic or carbonic 2D materials with periodically ordered structures is still an important bottleneck issue to be addressed. The exhibition of the expected properties of the building segments is highly related to their molecular arrangement in the 2D plane, which can also be affected by the synthesis process. Therefore, it is essential to give a comprehensive review focusing on the correlation between the preparation methods and the characteristic properties of functional 2D materials.

In this review, we discuss the preparation strategies to fabricate functional 2D materials prepared from molecular precursors. An overview of key issues for the design, fabrication, and application of 2D material systems will be presented to readers. The general principles referring to chemical structure design, functionalization, and the related effect on the basic

properties will be introduced. The detailed preparation method and assembly strategy of functional 2D materials will be presented. Combined with traditional assembly methods, some new-emerging preparation strategies comprehensively take advantage of the tailoring ability of covalent bonds and controlled assembly *via* supramolecular interaction. Then we will outline some recent applications of 2D materials in different kinds of devices. The structure–performance correlation of integrated devices will be discussed.<sup>38,54,61,66,75–88</sup> Finally, a brief perspective on future research directions for the preparation of functional 2D materials will be discussed. Structure design and assembly control are two powerful methods to fabricate innovative functional 2D materials.

## 2. Synthesis and functionalization

In general, the preparation strategies for 2D materials can be divided into top-down and bottom-up methods.<sup>31</sup> In the aspect of the top-down approach, the stripping method plays an important role, which obtains 2D materials through expanding the layer spacing of layered materials.<sup>89–91</sup> Compared to the top-down method, the bottom-up method has a wider application scope, which can obtain various kinds of 2D materials by designing specific precursors and utilizing various chemical reactions.<sup>92</sup> The basic research on the design, self-assembly, aggregation structure, and properties of advanced functional molecular systems have been carried out in the past decade.<sup>93–95</sup> A variety of crucial key factors including precursor design, coupling conditions, and post-treatment have been investigated. The careful selection of appropriate preparation methods can provide the opportunity to exhibit the characteristic properties of the building blocks for 2D materials. And effective functionalization can enrich the applications for 2D materials.<sup>82,96–99</sup> In this section, we will focus on the preparation and assembly of functional 2D materials, which can be prepared to start from the corresponding precursor molecules (Fig. 2).

### 2.1 Precursor design

Benefiting from the structural variety of organic molecules, the precursors can be linked through covalent or non-covalent bonds, which extensively influences the exhibiting regularity and stability of as-prepared 2D materials.<sup>100</sup> In 2010, starting from a new perspective of synthetic methodology, Li's group successfully fabricated 2D graphdiyne (GDY), which is the first all-carbon material obtained through synthetic chemistry in the world, giving birth to a new member of the carbon material “family”.<sup>101,102</sup> After the pioneering work, GDY based materials have been prepared in a large area to realize the scale preparation. The related application research has been systematically carried out.<sup>38,66,78–86</sup> At the same time, it has promoted the development of 2D carbon materials science and brought about bright opportunities for the further development of functional 2D material.<sup>103</sup> Following this work, varieties of GDY analogues have been synthesized *via* precursor design. By introducing different kinds of heteroatoms and functional groups, the



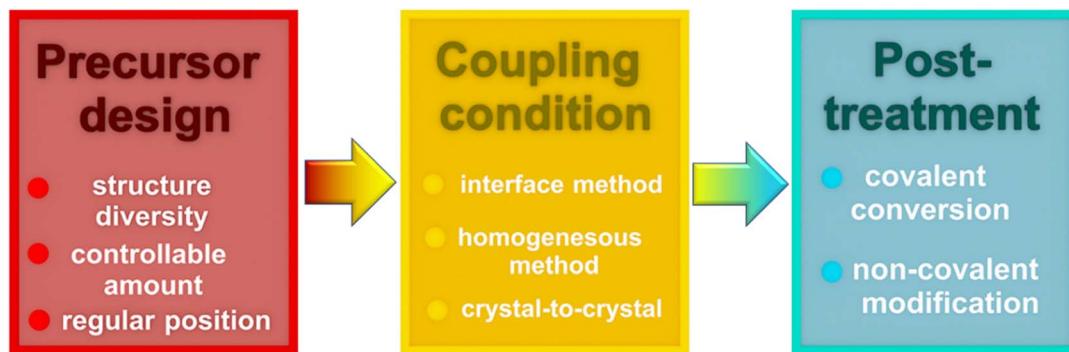


Fig. 2 Synthesis strategy for functional two-dimensional materials.

structural diversity of GDY is extremely expanded. For instance, Zhou *et al.* designed and synthesized a precursor, 1,3,5-triethyl-2,4,6-triphenyl-benzol, to participate in the coupling reaction instead of hexaethylbenzene (HEB).<sup>94</sup> Because of the supramolecular interactions between the precursor molecules, the layers on the surface of the copper foil kept growing laterally and eventually formed a layered GDY analogue (Fig. 3a). Apart from functional groups, heteroatoms can be doped into functional 2D materials with a controllable amount and fixed position. The uniform distribution of heteroatoms plays an important role in regulating the coupling process, aggregation structure, and physical properties of as-prepared products.<sup>81,104–107</sup> Due to the different intrinsic characteristics of the doped heteroatoms, there will be quite a different bonding environment around them. Thus, heteroatom doping

can effectively adjust the reaction process and adjust the properties of materials. Through chemical structure tailoring, the premise of preparing small molecules with different structures, combined with the advantages of “bottom-up” chemical preparation, can be prepared with different structural properties of functional 2D materials. Therefore, the introduction of heteroatoms is a very feasible strategy to regulate the structural morphology and corresponding physical and chemical properties of 2D materials.<sup>108,109</sup> The adjustable structures will provide an idea for the development of novel response materials. Most recently, Li and co-workers have fabricated dynamically adaptive 2D materials containing extended phosphine–acetylene rings through precursor design (Fig. 3b–f).<sup>106</sup> The introduction of linear acetylene phosphine units ensures structural flexibility compared to all-carbon 2D materials and lays the foundation for the synthesis of dynamic phosphate-containing 2D structures. Although the p–π conjugation is not significant in most trivalent phosphorus π systems with a pyramid structure, in P-GDY the lone pair electrons of phosphorus atoms are strongly involved in delocalization under the influence of interlayer van der Waals forces.

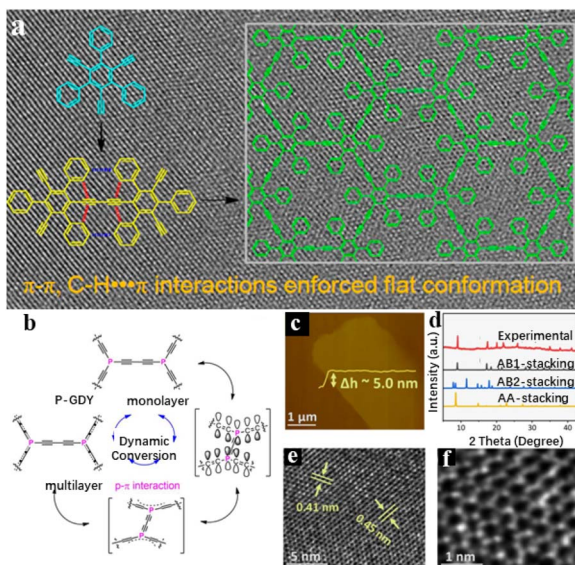


Fig. 3 (a) Schematic representation of non-covalent interactions affecting the conformation of the precursors during the synthesis of GDY analogue Ben-GDY. Adapted from ref. 94. Copyright 2019, American Chemical Society. (b) Dynamic conversion between monolayer GDY and multilayer GDY by p-π interaction. (c) AFM, (d) XRD, (e) and (f) HR-TEM images of P-GDY. Adapted from ref. 106. Copyright 2022, American Chemical Society.

## 2.2 Coupling conditions

The diversity of precursor structures is a prerequisite for the structural diversity of functional two-dimensional materials. And suitable reaction conditions are necessary for the preparation of functional two-dimensional materials with a determined structure. The most recent reports on synthetic 2D materials have confirmed that the restriction of the reaction types can be made up by effective synthetic methods, like interfacial synthesis, homogeneous phase approach, and crystal-to-crystal method.<sup>111</sup> In this section, we will introduce the recent advance in the aspect of synthetic methods.

**2.2.1 Interface method.** The development of surface synthetic chemistry demonstrates the compelling combination of organic chemistry and surface sciences. In the case of synthetic 2D materials, the interfacial method provides a reliable platform that can efficiently control the in-plane molecular arrangement orderliness and out-plane packing mode of as-prepared products.<sup>112</sup> The cross-link precursors with multiple reaction sites react at a spatially limited interface, such as

crystalline solid surface, liquid–liquid interface, and liquid–gas interface, *etc.* Until now, many independent organic or carbonic 2D materials have been prepared through different interface methods. Surface synthesis of 2D polymers can be carried out on solid surfaces with different environments, including under ultra-high vacuum (UHV), liquid/solid interfaces, and vapor/solid interfaces. The typical solid template is usually a polycrystalline metal substrate such as Cu, Ag, and Au.<sup>92</sup> Some of these metals can also act as catalysts to activate the polymerization of organic precursors. It is an effective strategy for the preparation of 2D networks with periodic structures on solid surfaces under UHV conditions.<sup>116</sup> In this field, small 2D polymer fragments are typically generated under UHV conditions and their 2D nanostructures are imitated by scanning tunnelling microscopy (STM). Due to the low mobility of the precursor on the solid template under UHV conditions, only the inferior reactivity can be exhibited in a small domain with tens of nanometres. Optimizing the interaction between nucleation and growth can realize substantial improvement.

In the liquid/solid interface reaction system, a solution containing organic precursors is added to a reaction solution containing a solid substrate, which is alternately soaked in one or more of the solutions containing the reactants.<sup>30</sup> The crystallization quality of polymerization is affected by the diffusion rate, concentration, and polymerization rate of precursors. Reaction on the surface of the solid involves several dynamic programs, including nucleation, diffusion, and growth. Generally, the precursor with a high diffusion rate on the substrates will improve the efficiency and selectivity of the reaction; crystal nuclei with low density and reaction processes with a slow rate are needed for generating a structure with high order. Although solid interfacial polymerization has the advantages of a controllable area and easy transfer of products, it still has some limitations in the fabrication of large-area 2D crystalline materials due to factors such as metal substrate etching. Thus, a metal–substrate catalytic reaction at the liquid/solid interface does not guarantee an efficient reaction. Slight corrosion of the substrate will produce a catalytic substance in the liquid medium, thus inducing solution-based reactions around the surface and resulting in aggregating nanostructures with different macroscale morphologies instead of expected 2D structures. Therefore, to obtain a 2D network at the liquid/solid interface, the catalytic activity and interfacial situation of the template should be carefully considered.<sup>112</sup> Currently, it is a challenge to fabricate ordered 2D materials in large areas, especially in the cases of the irreversible formation of C–C coupling on metallic templates with polycrystalline nature.<sup>117</sup> The experimental conditions should be carefully designed. Some newly developed strategies have been tried to fabricate 2D carbonic materials, which can be synthesized on a large scale and used in actual devices in the past decade. Like the classical synthesis method of 2D GDY films, copper foil acts as the substrate and catalyst, which was immersed in pyridine to catalyse the coupling of HEB.<sup>102</sup> After the evaporation of pyridine, a GDY film was obtained on the copper substrates.<sup>96</sup> When the template is replaced by other crystalline substrates such as sodium chloride, the coupling reaction of HEB can be

performed under the irradiation of microwaves to form few-layer GDY with ordered and crystalline interlayer packing forms (Fig. 4a).<sup>107</sup> Besides the reaction conditions, the reactivity and geometry of the selected precursor are crucial to fabricate crystalline 2D materials. For instance, a series of GDY analogues have been prepared by designing the corresponding precursor.

It is worth noting that the size of the solid-state template can also directly affect the morphology of the as-prepared 2D materials. For instance, Li and co-workers prepared high-quality GDY nanowires and ultrathin GDY nanosheets by replacing copper foil used in the synthesis of GDY films with copper nanowires (Fig. 4b).<sup>95</sup> In addition, it was found that GDY nanosheets are more easily formed at the crystal boundaries of Cu nanowires. The *in situ* synthesis of GDY nanosheets made the crystal boundaries stretched open, and the Cu nanowires were pulverized and scattered on the GDY nanosheets. Taking advantage of this, Li and his co-workers further synthesized GDY nanosheet anchored Cu quantum dots using polycrystalline Cu nanowires with crystal boundaries as the substrate and catalyst (Fig. 4c and d).<sup>79</sup> Furthermore, GDY can even grow on the surface of other 2D materials with ultra-thin thickness. In 2022, Li *et al.* used Cu(OAc)<sub>2</sub> as the catalyst and spread graphene in pyridine to synthesize a GDY/graphene/GDY sandwich-type 2D material.<sup>96</sup> Under the action of van der Waals interaction and lattice matching between GDY and graphene, GDY grew on both sides of graphene and finally formed a GDY/graphene/GDY sandwiched architecture (Fig. 4e and f).

The gas–liquid interface synthesis method usually refers to the polymerization of individual units at the air/water interface to form several or even a single layer of 2D nanosheets.<sup>118</sup> In general, small amounts of low-boiling organic solvents containing precursors are carefully spread at the aqueous interface. Keeping the system open, as the organic solvent evaporates, the precursor is exposed to the gas/liquid interface and crystallizes along the interface to form ultrathin nanosheets.<sup>119</sup> The gas–liquid method shows great advantages in the preparation of 2D materials with high crystallinity without pressure deformation. But in the process of crystallization, the interface is prone to various disturbances, so it is difficult to form large crystalline films. In recent years, scientists have made a lot of attempts to synthesize 2D organic or carbonic materials by using the gas–liquid method. The Langmuir–Blodgett (LB) technique is a promising method for preparing 2D materials by using the air–liquid interface.<sup>59</sup> This method required the use of amphiphilic molecules as raw materials. In the process of 2D material synthesis, the hydrophobic groups of amphiphilic molecules face the air, and the hydrophilic groups are inserted into the water, thus spreading out on the water's surface, forming a monolayer floating on the water. By confining the precursors to a 2D gas–liquid interface, the growth in the three-dimensional direction is avoided. Therefore, the LB method is one of the effective methods to form flat uniform large area 2D materials. In 2015, Dong *et al.* used the LB method to prepare novel 2D supramolecular polymer (2D SPs) monolayers at the air/water interface (Fig. 5a).<sup>110</sup> The precursors were spread over the aqueous surface and compressed into a dense film. 2D supramolecular polymerization was triggered with the diffusion



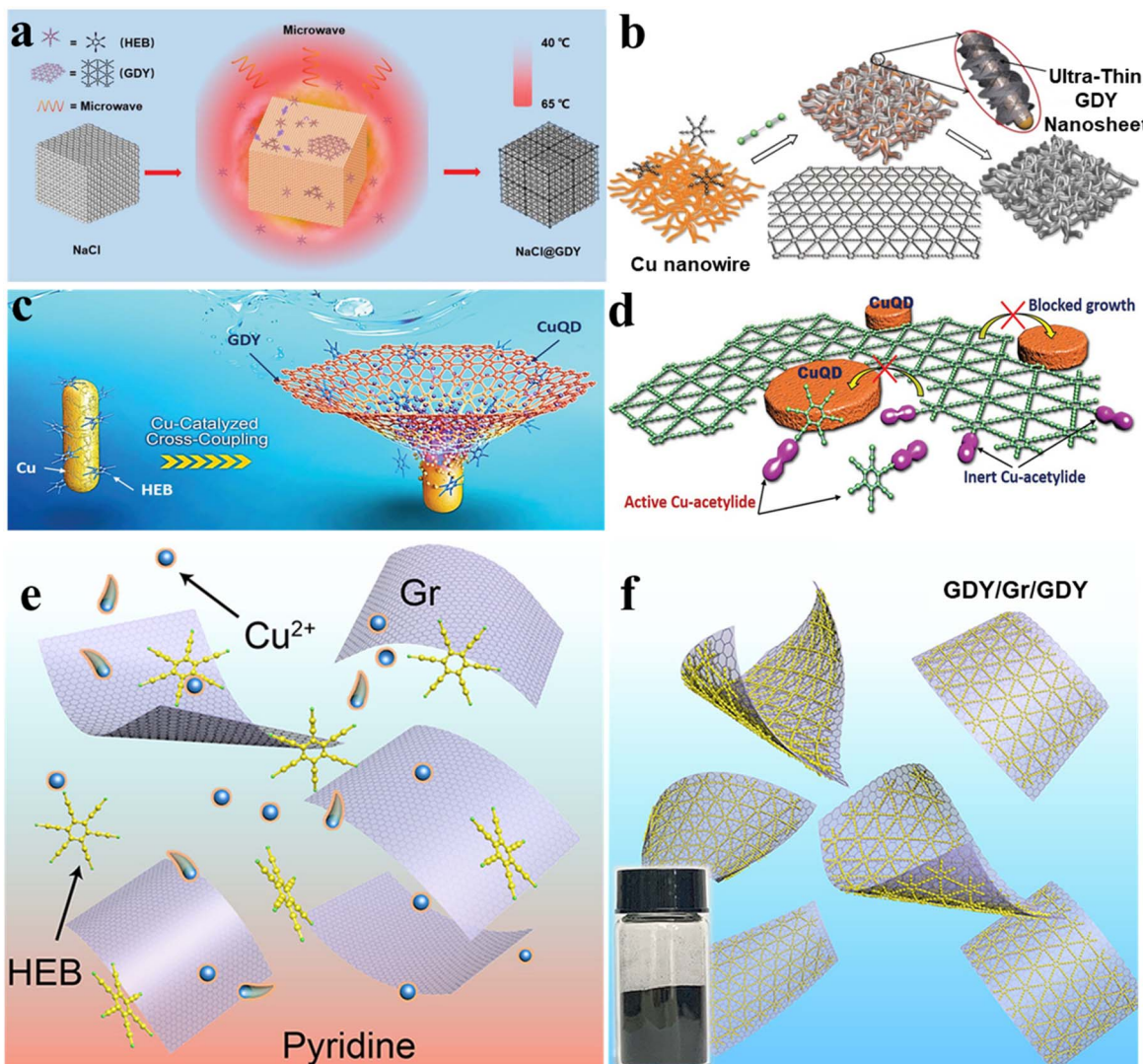
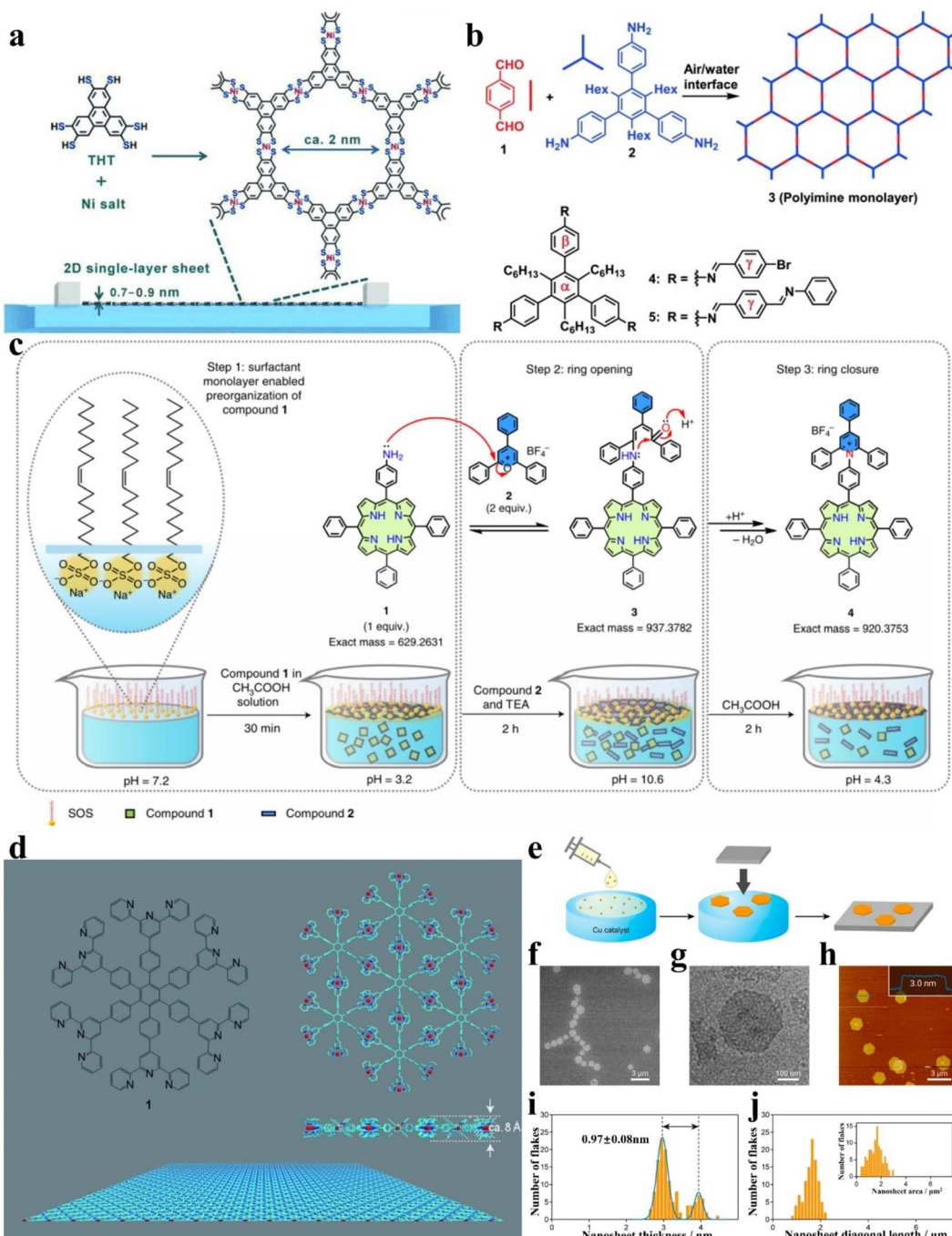


Fig. 4 Synthesis on the surface of the solid crystal with a wide scale range. (a) Synthesis schematic of crystalline GDY on sodium chloride crystals. Adapted from ref. 107. Copyright 2020, John Wiley & Sons. (b) The structure of ultra-thin GDY nanosheets grown on copper nanowires. Adapted from ref. 95. Copyright 2018, John Wiley & Sons. (c and d) The formation of Cu quantum dot loaded GDY (CuQD@GDY) because of the spontaneous splitting of Cu nanowires. Adapted from ref. 79. Copyright 2020, John Wiley & Sons. (e and f) Synthesis schematic of the GDY/Gr/GDY sandwiched architecture. Adapted from ref. 96. Copyright 2022, American Chemical Society.

of catalytic nickel ions in the aqueous phase. Coincidentally, Dai *et al.* also synthesized a 2D material starting from precursors with aromatic triamine and dialdehyde building blocks (Fig. 5b).<sup>111</sup> The designed precursors possess three hydrophobic *n*-hexyl groups and three hydrophilic amino groups so that the phenyl rings anchored by the three hydrophilic amino groups stay at the interface. Then the two aldehyde groups of terephthalaldehyde reacted with the amino group of 1,3,5-trihexyl-2,4,6-tris(4-aminophenyl)benzene to form an imine-linked 2D covalent monolayer. As for the non-amphiphilic molecular precursors, they can be flattened at the gas–liquid interface by other means of interaction, such as electrostatic interaction, complex effect, and conjugated interaction.<sup>112,119</sup> For example, in 2022, Wang *et al.* prepared charged 2D polymer single crystals by using electrostatic interaction between the protonated

compound 5-(4-aminophenyl)-10,15,20-(triphenyl)porphyrin and the anionic head groups of monolayer surfactant sodium oleyl sulphate (SOS) to make the precursor lay flat underneath the SOS monolayer and then carrying out the irreversible Katritzky reaction with 2,4,6-triphenylpyrylium tetrafluoroborate by controlling the pH value (Fig. 5c).<sup>120</sup> Bauer *et al.* confined the terpyridine-based  $D_{6h}$ -symmetric monomer to an air–liquid interface and then the monomer was polymerized into 2D free-standing, monolayered organometallic sheets by complexation between the monomer and metal ions (Fig. 5d).<sup>112</sup> In addition, Matsuoka *et al.* prepared thin GDY nanosheets by the gas–liquid interface method.<sup>64</sup> Under an inert argon atmosphere, a very small amount of HEB dissolved in methylene chloride/toluene mixture solution was added dropwise onto the surface of the aqueous solution containing the copper catalyst.





**Fig. 5** Gas–liquid method. (a) The 2D supramolecular polymer single-layer sheets are formed by the coordination of THT monomers and nickel ions. Reproduced with permission from ref. 110. Copyright 2015, John Wiley & Sons. (b) Synthesis of the 2D covalent organic monolayer formed by reversible imine bonding. Reproduced with permission from ref. 111. Copyright 2016, John Wiley & Sons. (c) Synthesis schematic of 2D polymer single crystals. Reproduced with permission from ref. 120. Copyright 2022, Springer Nature. (d) Structure of organometallic monolayer sheets and the monomer. Reproduced with permission from ref. 112. Copyright 2011, John Wiley & Sons. (e) Synthesis of GDY nanosheets at the gas/liquid interface. (f) SEM, (g) TEM, and (h) AFM of the GDY nanosheets on the HMDS/Si (100) substrate. (i) and (j) The thickness and size of GDY nanosheets. Reproduced with permission from ref. 64. Copyright 2017, American Chemical Society.

With the evaporation of the organic solvent, HEB polymerizes at the gas-liquid interface under the catalytic action of Cu and finally formed a GDY nanosheet (Fig. 5e-j). Different from the gas-liquid interfacial polymerization method which formed after the volatilization of low boiling point organic solvent, the

liquid-liquid interfacial polymerization method uses two kinds of immiscible liquid phase interfaces as the template for the growth of ordered 2D materials.<sup>120</sup> As reactants, the metal ions and the organic precursors dissolved in the aqueous phase and the organic phase, respectively. Under the influence of the

diffusion rate, the coupling reaction occurred at the interface of a few nanometres in thickness and formed a 2D material film with good crystallinity. In this method, the solubility of the reactants in organic and inorganic solvents is the key to the method. In 2019, Li and co-workers prepared free-standing 2D conjugated covalent organic framework (COF) films by the liquid–liquid interface method.<sup>117</sup> As shown in Fig. 6a, the inorganic base was dissolved in the aqueous phase and the water-insoluble components including the palladium catalyst, aryl halide, and aryl boronic were dissolved in the organic phase. Then the components of the two phases came into contact at the interface and started the Suzuki reaction eventually forming 2D COF films. Similarly, through the liquid–liquid interface method, Wang *et al.* constructed a water/organic phase interface by dissolving the metal precursor  $\text{Ni}(\text{OAc})_2$  in water and the organic linker terephthalic acid (1,4- $\text{H}_2\text{BDC}$ ) in a mixed organic solvent of *N,N*-dimethylacetamide (DMAc) and trichloromethane ( $\text{CHCl}_3$ ).<sup>118</sup> Due to immiscibility, organic solvent and water form a liquid–liquid interface at the

interface of the two solvents. Then a lot of light-green metal-organic framework nanosheets (MOF NSs) were formed at the interface between the two phases (Fig. 6b). GDY-based 2D materials can also be prepared by the liquid–liquid interface method. Matsuoka *et al.*<sup>64</sup> prepared GDY nanosheets by the liquid–liquid interface method. In the liquid–liquid system, the upper aqueous phase contained  $\text{Cu}(\text{OAc})_2$  and pyridine as catalysts, and the lower organic phase was dichloromethane containing monomer HEB. At the interface, HEB monomer was coupled with the copper catalyst to produce GDY nanosheets. By changing monomers in the lower organic phase, 2D heteroatom-doped GDY can also be prepared. For example, Kan *et al.* prepared nitrogenous GDY films, by designing a nitrogenous monomer and using it to replace the HEB monomer in the dichloromethane organic phase under the water/ $\text{CH}_2\text{Cl}_2$  interface.<sup>123</sup> It is important to note that the growth rate of 2D films depends on the diffusion rate of two solvents in two solvents. In addition, the coupling process of 2D material films can be controlled by adding an intermediate layer in the middle of the

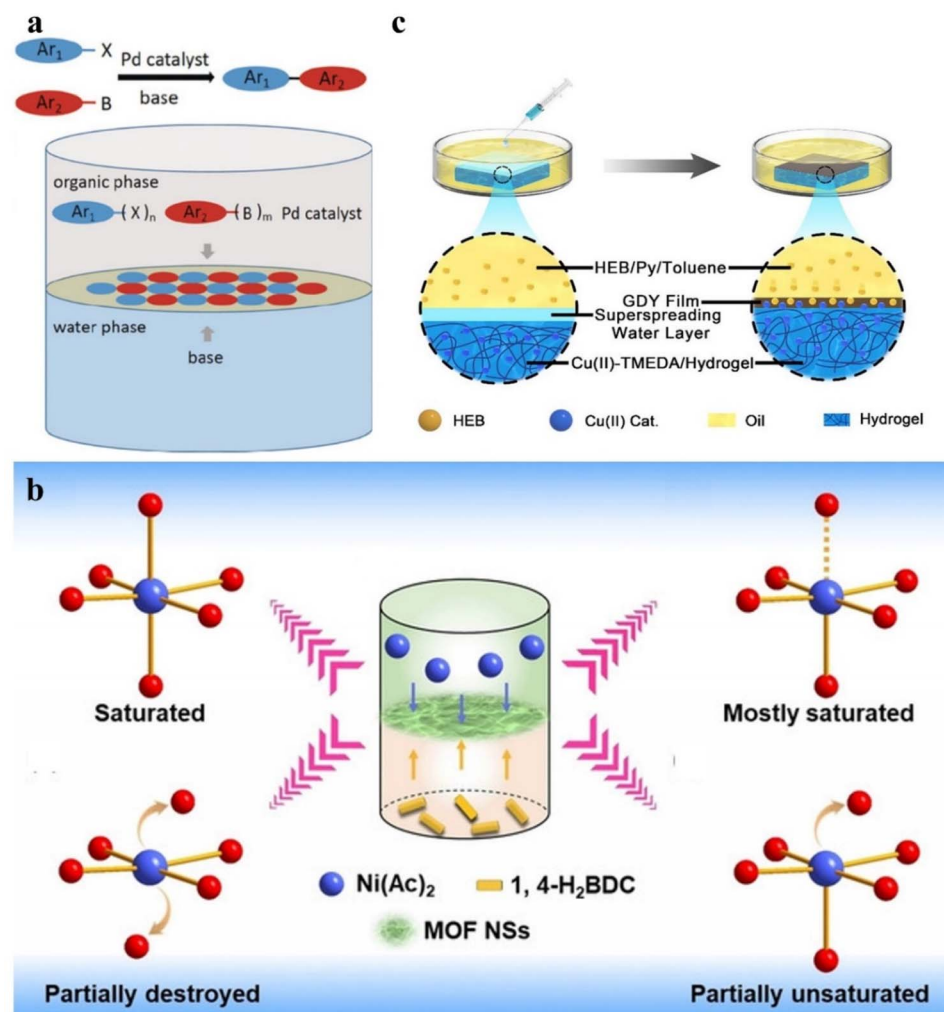


Fig. 6 Liquid–liquid method. (a) Synthesis of 2D COF films through the Suzuki reaction at the liquid–liquid interface. Reproduced with permission from ref. 117. Copyright 2019, John Wiley & Sons. (b) The preparation method of Ni MOF nanosheets. Reproduced with permission from ref. 118. Copyright 2021, John Wiley & Sons. (c) Superspreading interfacial contact between the organic solvent and hydrogel. Reproduced with permission from ref. 119. Copyright 2018, American Chemical Society.



two-phase interface, mainly because the intermediate layer is capable of slowing the premature diffusion of the reactants.<sup>124–126</sup> The existence of an intermediate layer is important because it avoids rapid mixing of precursors and allows them to spread slowly, which is beneficial to form better crystallinity. On the other hand, the reaction rate can also be sped up at a toluene/hydrogel interface, which shows super-spreading interfacial contact (Fig. 6c).<sup>119</sup>

Based on the above discussion, the interface method has the advantages of simple operation and mild reaction conditions.<sup>121,127,128</sup> Meanwhile, some key issues remain to be addressed referring to synthetic conditions besides the precursor design. For instance, detailed reaction conditions such as reaction temperature and pH limit the application range of some chemical reactions.<sup>129</sup> In addition, a systematic investigation of reaction processes and mechanisms, such as the interaction and diffusion of precursor molecules at the interface, will further improve the controlled synthesis of 2D materials with ordered structural periodicity. One of the most represented reports refers to the van der Waals epitaxial growth of GDY with few layer and ordered ABC stacking on the surface of a graphene template (Fig. 7a–e).<sup>121</sup> The coupling process can be controlled more accurately through the application of the technique of continuous flow synthesis (Fig. 7f–h).<sup>122</sup> The precise control of experimental conditions is conducive to further understanding of the role of weak interaction in interfacial reactions.

**2.2.2 Homogeneous growth.** Homogeneous growth of functional 2D materials refers to the direct synthesis in solution without any substrates of interfacial assistance.<sup>133,134</sup> The precursor structure design for efficient coupling is very strict. First, the configuration must be rigid, which can facilitate the coupling reaction in the 2D direction. Second, steric hindrance and electrostatic interactions are essential to avoid stacking

between layers. The synthesis of 2D materials can be achieved by pre-assembly in the homogeneous solution phase.<sup>135</sup> For example, Wang *et al.* prepared fully sp<sup>2</sup>-carbon conjugated 2D covalent organic frameworks (COFs) which contained benzobisthiazole units and were connected by cyano-vinylene linkages through a reversible Knoevenagel polycondensation reaction (Fig. 8a).<sup>127</sup> In the synthesis of these 2D COF materials, the reaction condition control was very important. Notably, one advantage of the homogeneous growth approach is that neither stripping nor interfacial transfer is needed, which is beneficial to the further application of as-prepared 2D materials.<sup>113–115,123</sup> Following this approach, functional 2D materials with a high crystallinity and specific surface area have been prepared in large quantities through typical reversible reactions (Fig. 8b).<sup>128,136</sup> Nevertheless, it is also worth paying attention that the reversibility of dynamic covalent bonds in 2D materials will unavoidably weaken the stability of the materials.<sup>130–132</sup> Thus, the conjugate degree and stability of the above 2D material are unavoidably inferior to the existence of heteroatom-contained or non-covalent linking groups.<sup>63</sup>

On the other hand, the formation of carbon–carbon bonds with a low reversibility reaction can improve the conjugation and stability of 2D materials, but the as-prepared materials such as 2D conjugated polymers also suffer from structural defects and irregular packing.<sup>137</sup> Therefore, the preparation of functional 2D materials with high crystallinity, high conjugation, and excellent stability is a major challenge in the related field.<sup>138,139</sup> Therefore, new research ideas and methods to solve the related important scientific problems and difficulties need to be put forward continuously.<sup>68</sup> Zeng *et al.* prepared a stable 2D polymeric material by a 2D irreversible polycondensation reaction.<sup>63</sup> As shown in Fig. 8c–h, acid chloride and melamine with C<sub>3</sub> symmetry undergo an amide condensation. In the condensation process, a strong conjugation effect can inhibit

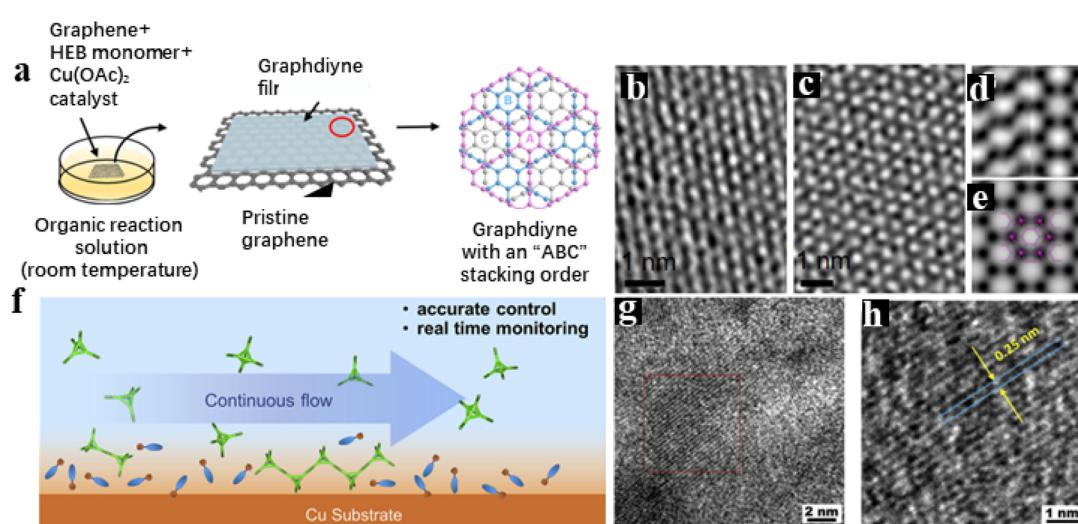
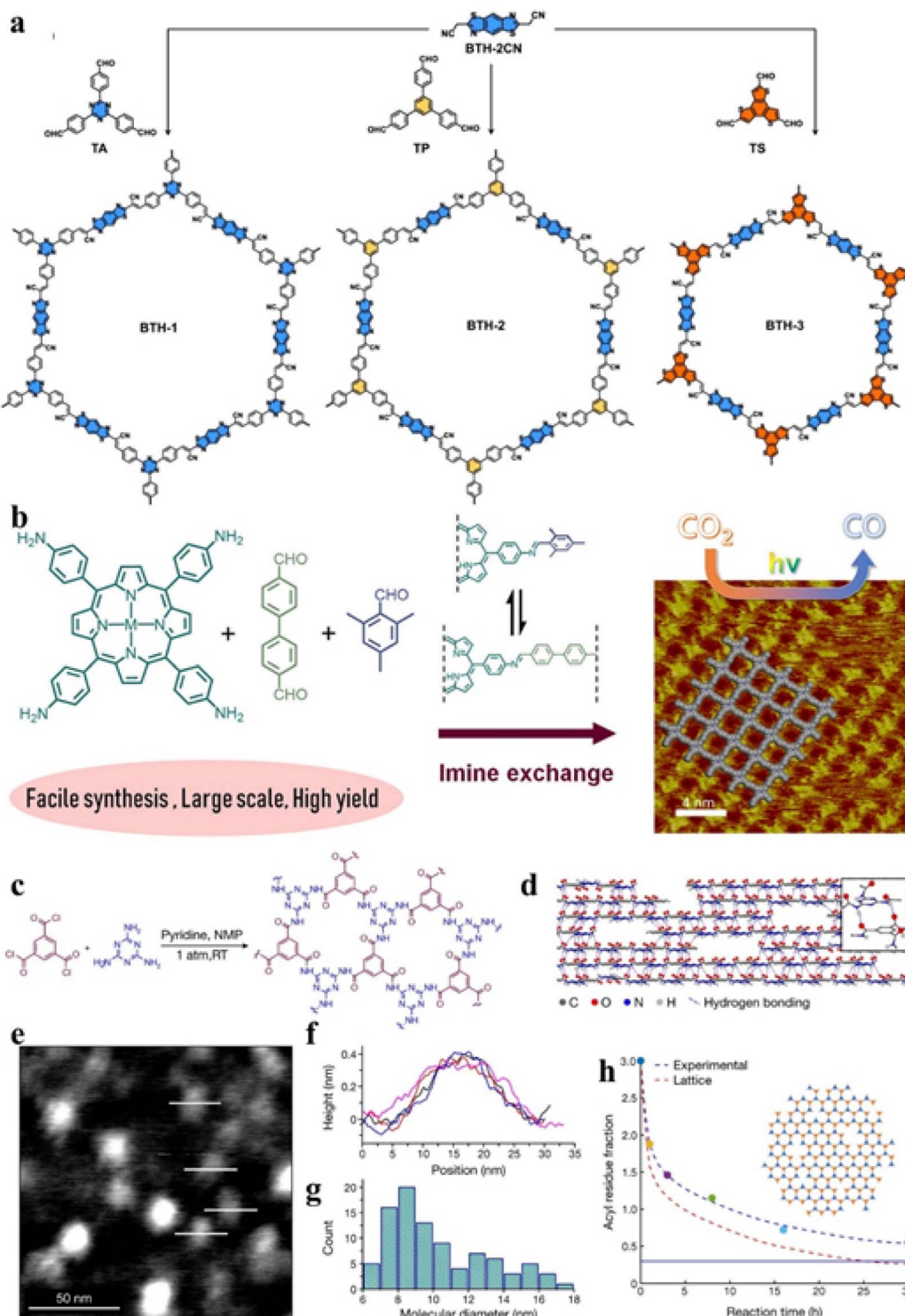


Fig. 7 Some innovations in interface methods. (a) Solution-phase van der Waals epitaxy growth of ultra-thin single crystal GDY films on graphene. (b)–(e) Stacking mode and lattice information of the GDY. Adapted from ref. 121. Copyright 2018, American Association for the Advancement of Science. Synthetic process on a continuous flow surface (f) and HRTEM images (g and h) of COF films. Adapted from ref. 122. Copyright 2022, Elsevier.





**Fig. 8** Examples of the preassembly in solution strategy. (a) Synthetic routes and structures of three vinylene-linked 2D COFs (BTH-1, 2, and 3). Adapted from ref. 127. Copyright 2022, Springer Nature. (b) A facile synthetic route of imine-linked COF nanosheets on a large scale and in high yield. Adapted from ref. 128. Copyright 2019, American Chemical Society. (c) Synthesis of a 2D polyaramid (2DPA-1). (d) Structure of 2DPA-1. (e) Image of TMS-2DPA-1 high-resolution AFM. (f) and (g) The thickness and size of TMS-2DPA-1. (h) Variation of molecular aggregation with reaction time. Adapted from ref. 63. Copyright 2022, Springer Nature.

rotation in an out-of-plane direction, resulting in the formation of 2D polyaramids. At the same time, interlayer hydrogen bonds or van der Waals forces made the material continuously extend

in the 2D direction. Due to the inert amide linkage, the 2D polymer material had strong mechanical and chemical stability and high processability.<sup>72</sup> Although there are many limitations

in structure design, homogeneous growth is an effective way to synthesize two-dimensional materials in large quantities.

**2.2.3 Crystal-to-crystal method.** The strategy of single crystal to single crystal (SCSC) refers to the method of polymerizing crystalline precursor into 2D material single crystals by particular reactions such as photochemical cycloaddition.<sup>140</sup> Compared to the other methods, the 2D materials obtained by the SCSC method exhibit higher quality, a smaller number of defects, and larger size, which is more conducive to the application of 2D materials in practical devices.<sup>140–142</sup> In fact, SCSC conversion can be regarded as another type of topological chemical reaction that can be used to construct 2D layers.<sup>143</sup> It is worth noting that the SCSC method had two difficulties. Firstly, it is difficult to control the stripping of 2DP single crystals; secondly, SCSC transformation is difficult to achieve, because the monomer crystallization process was difficult to predict; the contractions and expansions upon the monomer polymerization easily lead to single crystal cracking.<sup>144–146</sup>

In the pioneering work, Sakamoto and colleagues designed a molecule with tripod shape showing response to light.<sup>143</sup> The single crystal structure of the monomer reveals two advantageous characteristics of 2D polymerization: (1) the stratified structure ensures the separation of xylene anthracene units, thus preventing cross-linking across layers; (2) hexagonal stacking within each layer, in which each of the three

anthracene units of a precursor exists close to an alkyne group in an adjacent monomer molecule, allows the interlamellar [4 + 2] cycloaddition to occur. Similar demonstrations have been made using different molecular designs through organization within crystals. King and colleagues have succeeded in synthesis and crystallization which contains anthracene units.<sup>144</sup> The single crystal lattice of long-range order and the ultimate structure in the process of the organization provide a solid functional group and location precision, to build a highly ordered 2D layered crystal. It should be noted that optical crosslinking induces crystal-to-crystal conversion by dimerization of [4 + 4] anthracene, resulting in a layered 2D polymer that can be stripped off into monolayers by solvent treatment. Zhao and co-workers designed the monomer M1 containing triazine as the core and styryl pyridine as three arms to synthesize single-crystalline 2D materials by SCSC transformation based on photochemical [2 + 2]-cycloaddition.<sup>62</sup> As shown in Fig. 9a–i, the three functional arms of M1 were packed in a head-to-tail fashion at a distance of 3.919 Å which satisfies the geometry criterion of Schmidt and form a hexagonal plane tiling after the photochemical cycloaddition. The triazine units of M1 were easily protonated by acid, which can introduce interlayer repulsion, thus effectively realizing the exfoliation of 2DP single crystals. Then trifluoroacetic acid/γ-butyrolactone (TPA/GBL) was used to exfoliate 2DP single crystals in the liquid

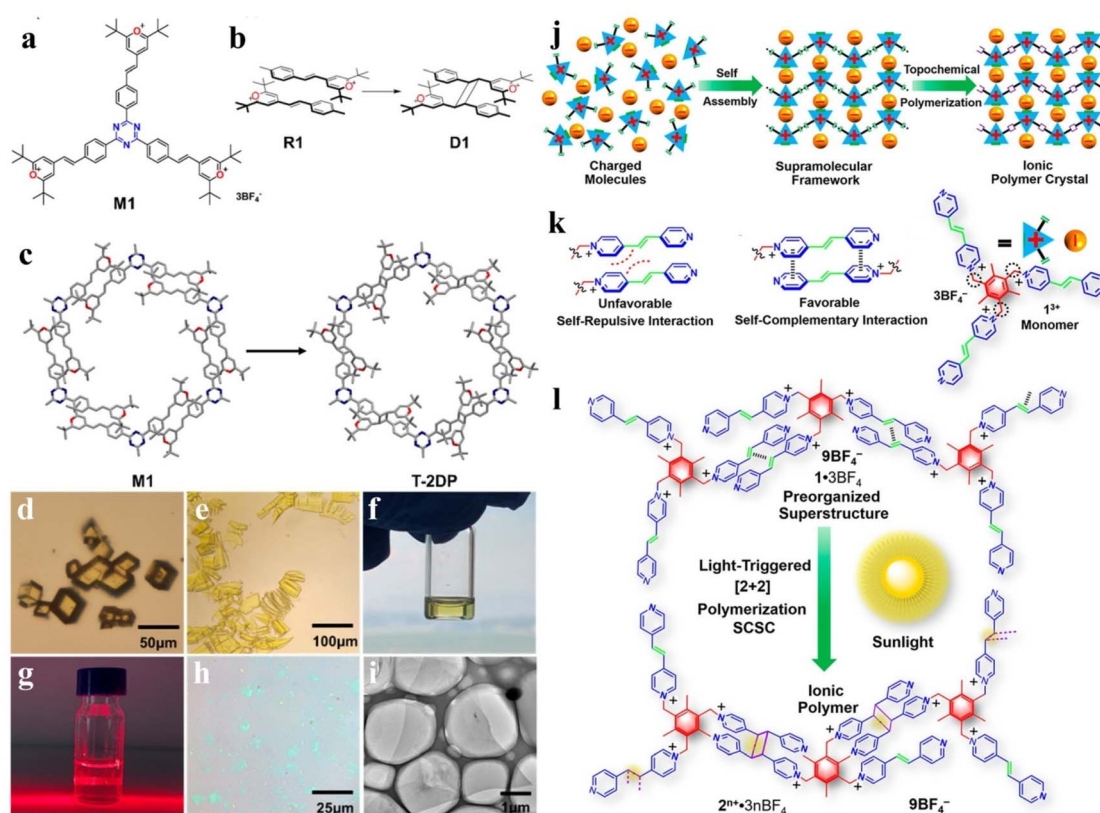


Fig. 9 Single crystal transformation strategy. (a)–(c) Synthesis of single crystal 2D polymer (T-2DP). (d) and (e) The shape of a T-2DP single crystal and exfoliated T-2DP single crystal. (f) and (g) The solution of T-2DP and its Tyndall effect. (h) Optical microscope image of T-2DP. (i) TEM of a T-2DP flake. Adapted from ref. 62. Copyright 2021, American Chemical Society. (j)–(l) The synthesis of a 2D lamellar sheet with sub-nanopores. Adapted from ref. 129. Copyright 2020, American Chemical Society.



phase, and finally got 2D nanosheets with a thickness of 0.7–0.8 nm and a single molecular film accounting for 80%. At the same time, the presence of GBL made the exfoliated 2DP layers have good dispersibility. In this work, the existence of triazine as a core is the key to solving the problem of 2DP single crystal exfoliation. The controllable synthesis of a single crystal polyelectrolyte material with perfect orthotic regularity was realized on a gram scale through the SCSC strategy by Stoddart and coworkers.<sup>129</sup> The design idea can be summarized as a two-step method including preassembly and *in situ* polymerization (Fig. 9j). The three-arm monomer self-assembles under charge to form a neatly arranged precursor single crystal (Fig. 9k). Under light irradiation, [2 + 2] photodimerization *in situ* occurs between monomer arms containing unsaturated bonds, which realizes direct conversion from solid monomer single crystals to polymer single crystals (Fig. 9l). In addition, the research team carried out liquid stripping of polyelectrolyte single crystals. 2D monolayer polyelectrolyte films were obtained by mixing GBL at 50 °C for five days. The thickness of the monolayer measured by atomic force microscopy (AFM) is 1 nm, which is consistent with the data obtained from the crystal structure. The strong ionic bond between the main chain and the ligand ion effectively maintains the highly ordered interchain structure, which makes the stripping of the stable monolayer possible. Crystal-to-crystal is an efficient method to obtain a 2D material with a definite crystallinity and structure.

### 2.3 Post-treatment

The varieties of designed precursors lead to the diversity of 2D materials. A suitable coupling method is essential for 2D materials with a well-defined structure. And post-treatment could endow 2D materials with well-defined structures with a new function. The strategies for post-treatment, either covalent conversion to tune the properties of 2D materials or non-covalent modifications to extend the properties, greatly expand the applications of 2D materials.

**2.3.1 Covalent conversion.** Post-conversion of the linkage group can adjust the material dimension, morphology, topology regulation, composition, and so on. For example, some 3D materials can be transformed into 2D materials by eliminating interlayer interactions. Huang *et al.* prepared 3D pillared layer metal–organic frameworks (MOFs) by solvothermal reaction of 2,3-dihydroxy-1,4-benzenedicarboxylic acid ( $H_4\text{dhbdc}$ ) and  $\text{Co}(\text{CH}_3\text{COO})_2$ .<sup>65</sup> As shown in Fig. 10a, the 3D MOF was composed of wavelike  $\text{Co}(\text{CH}_3\text{COO})_2$  layers and  $H_2\text{dhbdc}_2$ -pillar ligands between the layers. These pillar ligands can be slowly oxidized *in situ* and removed in the electrolyte solution saturated with  $\text{O}_2$ , and the post-synthesis conversion can be accelerated by electrolysis. After the removal of the  $H_2\text{dhbdc}_2$ -pillars, the bulk 3D MOF was transformed into a 2D ultrathin nanosheet with folds, whose thickness was only 2 nm (Fig. 10b–g). In addition, post-conversion can also be achieved by using intramolecular hydrogen bonds through the ingenious design of molecular connectors with different substituent groups, exhibiting quite different topologies. For instance, tetrakis(4-aminophenyl)ethane (TPE-NH<sub>2</sub>) can be connected with 2,3-dihydroxyterephthal-aldehyde (2,3-DHTA) and

2,3-dimethoxyterephthalaldehyde (2,3-DMTA), respectively, to prepare two kinds of high crystallinity 2D COF materials.<sup>47</sup> Because of the intramolecular hydrogen bonds between –OH and –NH<sub>2</sub>, the C=C and C=N linkages of the COF composed of TPE-NH<sub>2</sub> and 2,3-DHTA have *cis* conformation. However, the C=C and C=N linkages of the COF composed of TPE-NH<sub>2</sub> and 2,3-DMTA have *trans* conformation (Fig. 10h).

Besides the non-covalent interaction, the post-conversion of 2D functional materials can also be performed by generating new covalent bonds through reactions. As shown in Fig. 10i, GDY doped with sp hybrid nitrogen was successfully introduced into the alkyne bond through the cycloaddition reaction.<sup>137</sup> DFT calculations indicate that sp-N has a high negative charge density, resulting in a higher positive charge density of adjacent carbon atoms. In another report, Wang *et al.* prepared two ultra-stable 2D frameworks containing a thienopyridine linker. The unstable imine bond is converted to conjugated linkages through an oxidative cyclization reaction.<sup>43</sup> In the cyclization process, the carbon atom thiophene segment is bonded to the carbon of the imine to obtain the thienopyridine segment. The super stability of the products can be ascribed to the strong  $\pi$ -electron-delocalized linkages of the thienopyridine units (Fig. 10j).

**2.3.2 Non-covalent modification.** Single metallic atom modification is a common-used strategy for the functionalization of 2D materials.<sup>147</sup> There are many methods to introduce metal atoms into 2D carbon-based materials, including pyrolysis, wet chemical synthesis, physicochemical vapor deposition, electrochemical deposition, and ball milling.<sup>6</sup> A variety of metallic atoms have been tried to anchor on 2D materials through the coordination or electrostatic interaction between 2D materials and metal atoms.<sup>148</sup> The electronic structure of 2D materials can be efficiently tuned, to adjust the intrinsic activity of 2D materials. In addition, the activity of the modified single atom can also enable 2D materials to show excellent performance in some fields, especially in catalysis. For example, through the electrochemical reduction method, Ni/Fe (Fig. 11a),<sup>54</sup> Pd (Fig. 11b),<sup>78</sup> and Cu (Fig. 11c)<sup>100</sup> can be anchored on the GDY films, which are grown on particular substrates such as carbon cloth. Due to the chemical interaction and electronic coupling between the single metal atom and the 2D GDY film, the transfer efficiency of charge between the carrier and the catalytic active site is greatly improved.<sup>149</sup> Therefore, the 2D materials modified with single atoms show excellent catalytic activity and stability in electrochemical catalytic reactions such as hydrogen evolution and nitrogen reduction.<sup>6</sup> On the other hand, metallic compounds can also be used as functional components to tune the properties of 2D materials. For example,  $\text{PtCl}_2\text{Au}(111)/\text{GDY}$  with atomically Pt species has been fabricated through an interesting two-step strategy (Fig. 12a).<sup>66</sup> In this method, the support GDY was first soaked in  $\text{H}_2\text{PtCl}_6 \cdot 6\text{H}_2\text{O}$  solution, and  $\text{Pt-Cl}_4$  was adsorbed on GDY. The resulting material was then immersed in  $\text{HAuCl}_4 \cdot 3\text{H}_2\text{O}$  solution.

The Au quantum dots were made to undergo epitaxial growth by electrodeposition using isolated  $\text{Pt-Cl}_4$  species. In this process,  $\text{PtCl}_2$  was uniformly inserted into the lattice of Au to form  $\text{PtCl}_2$  single atoms. The unique structure of  $\text{PtCl}_2\text{Au}(111)/\text{GDY}$  made it have good catalytic performance and stability in methanol



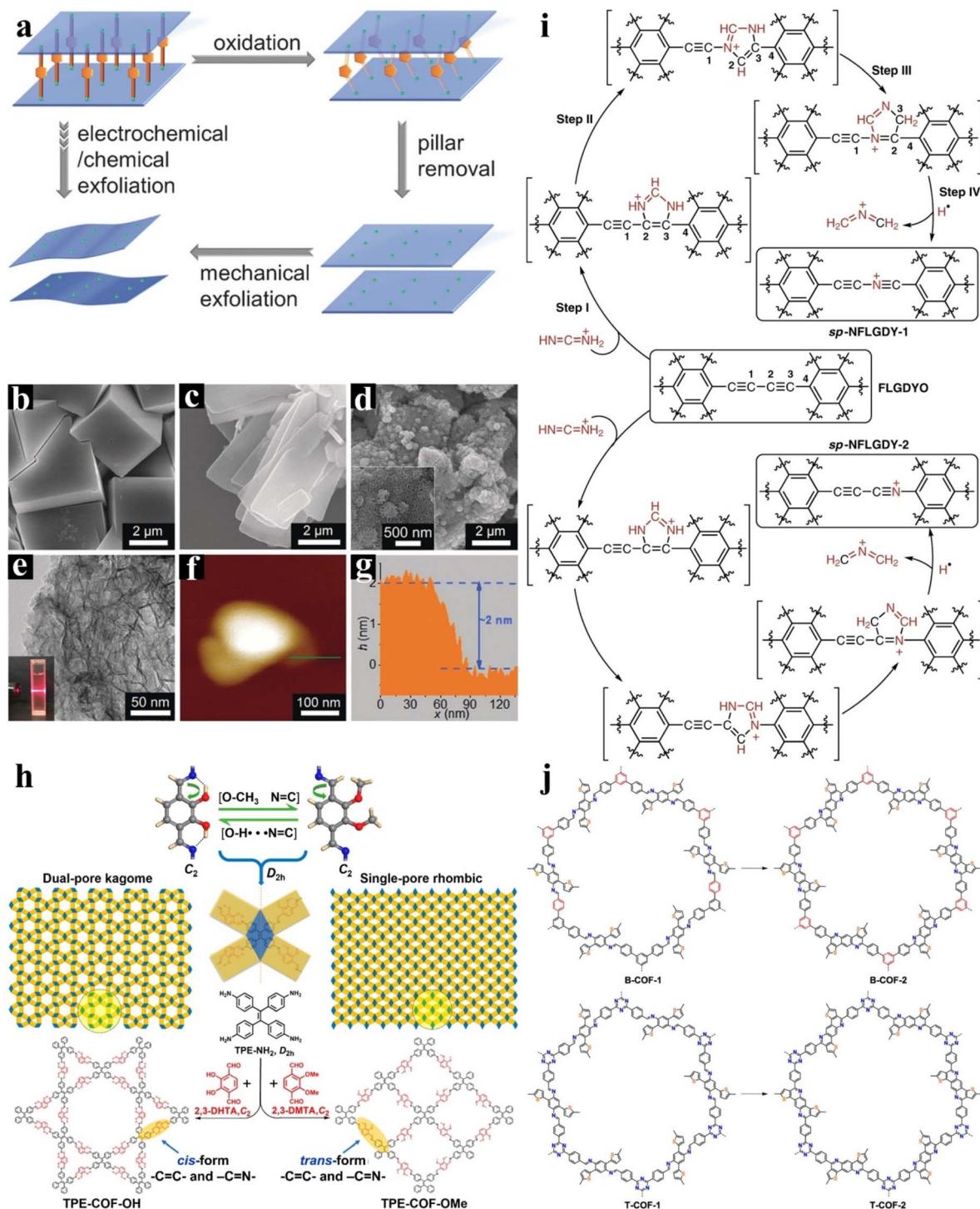


**Fig. 10** Post-treatment strategy. (a) A pillared-layer MOF removed pillar and exfoliated to prepare a 2D MOF. SEM images of 3D-Co (b), 2D-Co (c), and 2D-Co-NS (d). The TEM (e) and AFM (f) images of 2D-Co-NS. (g) The corresponding height analysis of 2D-Co-NS. Adapted from ref. 65. Copyright 2018, John Wiley & Sons. (h) Synthesis of TPE-COF-OH and TPE-COF-OMe with different topologies. Adapted from ref. 47 Copyright 2020, American Chemical Society. (i) Synthesis of few-layer sp-N-doped GDY. Adapted from ref. 137. Copyright 2018, Springer Nature. (j) Schematic of structural conversion from imine-linked COFs (B-COF-1 and T-COF-1) to thieno[3,2-c]pyridine-linked COFs (B-COF-2 and T-COF-2). Adapted from ref. 43. Copyright 2020, American Chemical Society.

oxidation reactions and ethanol oxidation reactions. Most recently, Gao *et al.* have developed a new concept of *in situ* controlled growth of double-layer heterogeneous interfacial

structures (GDY/RhO<sub>x</sub>/GDY).<sup>76</sup> The interfacial interaction between the carbonic and metallic components enables the catalytic material to have excellent charge transfer ability, excellent

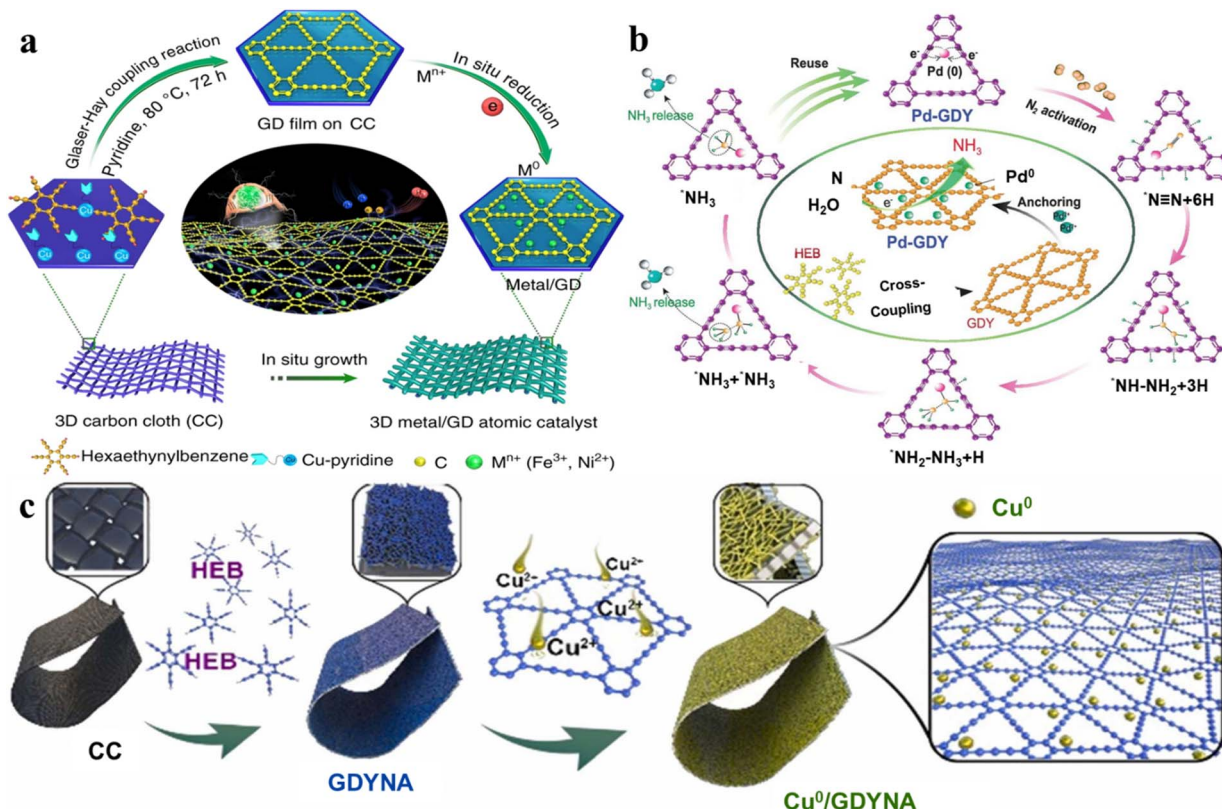


Fig. 11 Functional 2D materials loaded with a single atom or metallic compound. (a) Synthesis of Fe/GD and Ni/GD. Adapted from ref. 54. Copyright 2018, Springer Nature. (b) Synthesis of Pd-GDY and its reusability in electrocatalytic ammonia production. Adapted from ref. 78. Copyright 2021, Oxford Univ Press. (c) Synthesis of Cu<sup>0</sup>/GDYNA for nitrate reduction. Adapted from ref. 100. Copyright 2022, Elsevier.

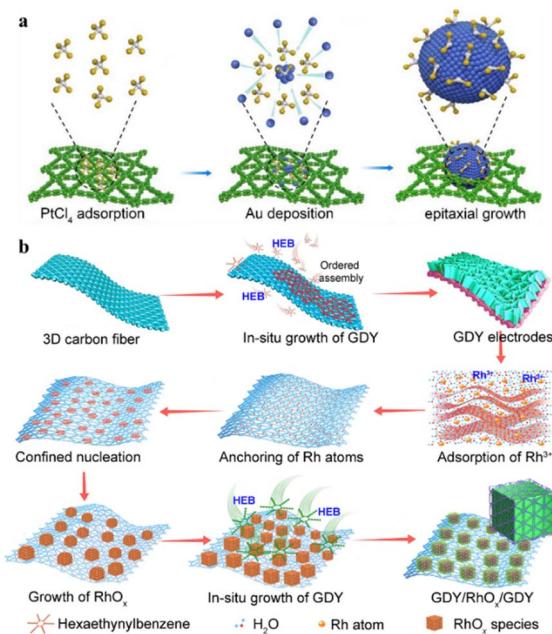


Fig. 12 (a) Synthesis of PtCl<sub>4</sub>Au(111)/GDY. Adapted from ref. 66. Copyright 2022, American Chemical Society. (b) Synthesis schematic of the GDY/RhO<sub>x</sub>/GDY electrodes. Adapted from ref. 76. Copyright 2022, National Academy of Science.

conductivity, an abundant number of active sites, and ultra-high electrocatalytic activity. The unique incomplete charge transfer phenomenon between the electron donor and acceptor at the catalyst interface endowed the catalytic system with ultra-high reactivity and selectivity (Fig. 12b). Furthermore, studies have shown that in metal monatomic carbon materials, metal atoms can be combined with N, O, S, P and other heteroatoms in the carbon support matrix through coordination bonds.<sup>105,107,150-153</sup> Therefore, charge transfer can occur between metal atoms and heteroatoms, thus affecting the electronic structure of 2D materials.<sup>154</sup> Based on the unique structural characteristics of the 2D material structure and the advantages of synthesis and preparation by the chemical method, the further introduction of metal single atoms and other components into heteroatomic-doped 2D materials is an extremely effective strategy to systematically regulate the structure and properties.<sup>103</sup>

### 3. Characteristic properties and related application

2D materials possess a single layer or a few layers of repeated units, which are fixed by enormous covalent or non-covalent bonds within the layer, and bounded by van der Waals forces among the layers.<sup>23,28</sup> The structural advantage enables the electron to only move freely in the 2D plane so that it's easy to

change the band structure and properties of 2D materials by stretching the lattice, causing defects, surface modification and thickness adjustment. Moreover, different 2D materials can be further stacked into heterogeneous structures through van der Waals forces, thus achieving the integration of different materials and properties. The characteristics of 2D materials enable them to show excellent performance in a variety of practical devices.<sup>42,155</sup> In this section, the up-to-date research progress is discussed from a viewpoint of the correlation between characteristic properties and related applications.

### 3.1 Mechanical properties

One of the most important cores of actuators is piezoelectric materials, which are usually polar and can be driven with high precision by applying a voltage to obtain a slight deformation.<sup>156</sup> This characteristic has made actuators an excellent tool for

achieving high precision positioning and equipped with cutting-edge instruments such as a scanning tunnelling microscope (STM). Thus, it can be said that piezoelectric materials have become a “smart muscle” to explore the micro-world. Even so, as mentioned above, achieving ultra-high precision localization at the subatomic scale remains extremely challenging. 2D materials have unique advantages in piezoelectric properties. While the key segments of 2D materials are compressed into a single atomic layer, the centre of symmetry disappears, which might induce outstanding piezoelectric properties compared to traditional bulk materials.<sup>157,158</sup> Notably, the exhibiting piezoelectric properties of 2D materials can be effectively improved through introducing hetero-atoms.<sup>157</sup> For example, the incorporation of sulphur hetero-atoms affects the structural symmetry of GDY, resulting in good piezoelectric properties of SGDY (Fig. 13a–f).<sup>156</sup> On the other hand, the outstanding strain behaviour of 2D materials is the

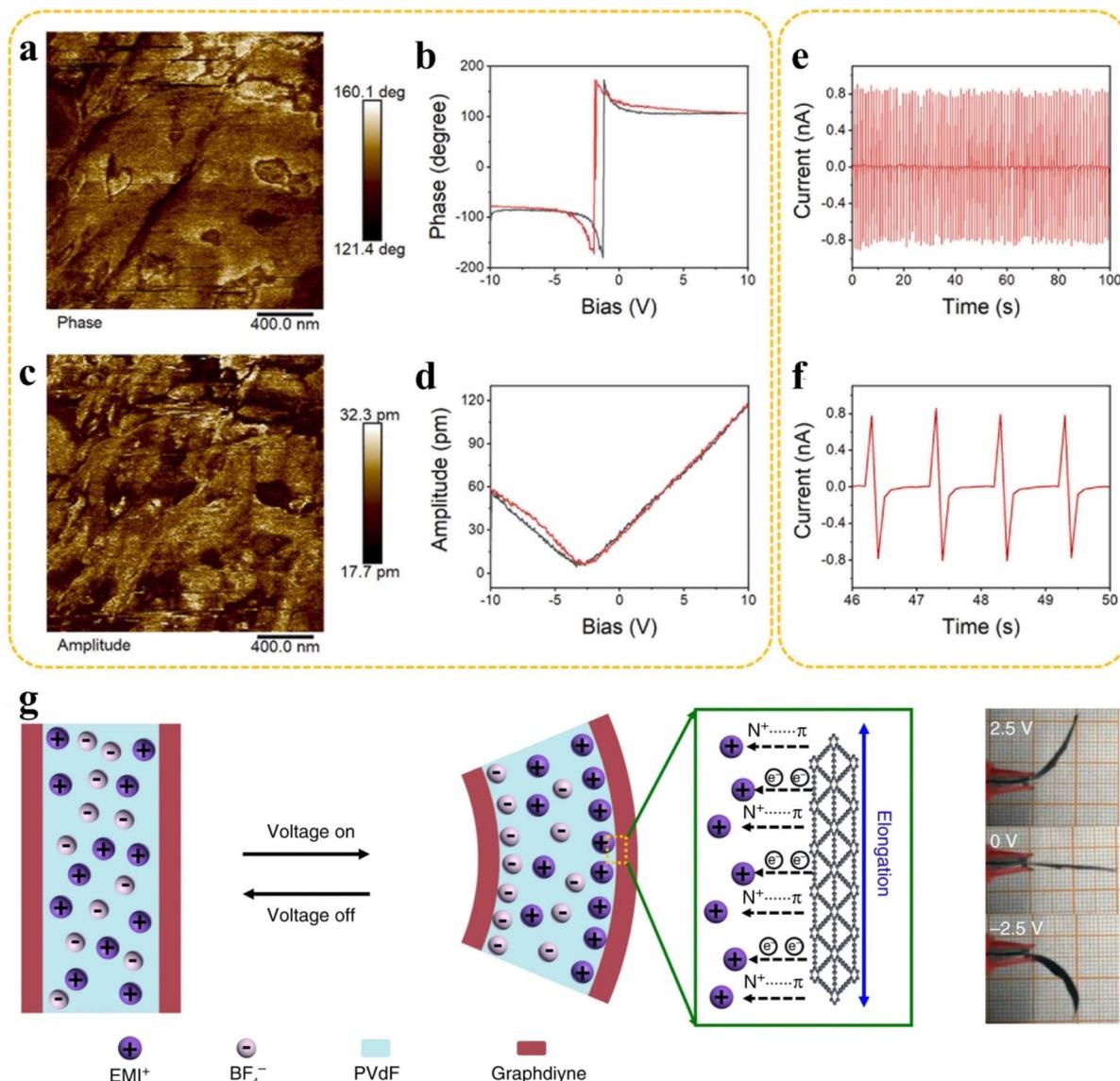


Fig. 13 Application of piezoelectric 2D materials. (a–f) Piezoelectric properties of the SGDY electrocatalyst. Adapted from ref. 156. Copyright 2022, Elsevier. (g) The actuation mechanism of a GDY-based flexible ionic actuator. Adapted from ref. 84. Copyright 2018, Springer Nature.



basis of their application in the corresponding piezoelectric devices. The deformation of 2D materials can also be realized by changing the internal bond length, which converted electrical energy into mechanical energy by utilizing the strain in the ion complexation process. Lu *et al.* prepared a complex actuator based on an ionic polymer and GDY, which converts electrical energy into mechanical energy by utilizing strains during ion complexation (Fig. 13g).<sup>84</sup> The electromechanical conversion efficiency is as high as 6.03%, which exceeds that of previously reported piezoelectric ceramics, shape memory alloys, and electroactive polymers. Moreover, the energy density is also comparable to that of mammal skeletal muscle and can be used in biomimetic devices such as artificial muscles.

### 3.2 Thermal properties

Thermoelectric materials based on the Seebeck effect and Peltier effect are a class of special materials which can directly convert heat energy and electric energy into each other.<sup>159</sup> They have outstanding advantages such as no noise, no pollution, and no need for long-term maintenance, which has attracted wide attention.<sup>160</sup> Due to the low efficiency of thermoelectric conversion, the application of traditional organic solid materials in flexible thermoelectric devices is greatly limited.<sup>161</sup> Recent studies have shown that low-dimensional materials can have higher thermoelectric conversion efficiency due to quantum confinement effects.<sup>162</sup> Therefore, the study of the thermoelectric properties of 2D materials has become an attractive research spot, which can not only provide powerful

theoretical support for alleviating the energy and environmental crisis faced by current society but also provide theoretical models for obtaining higher-performance thermoelectric materials.<sup>163</sup>

Generally, 2D materials have unique properties in thermal transport because of their different phonon dispersion relationship from bulk materials.<sup>164</sup> For example, in the long-wave approximation, the dispersion relationship of acoustic phonons with a bulk structure is linear, while the 2D structure presents an obvious parabola form, which will reduce the velocity of phonons and affect the scattering mechanism of phonons, thus affecting the heat transport properties of materials.<sup>165</sup> At the same time, with the decrease of dimensions, the influence of the interface will also be introduced, which makes 2D materials have proper thermal transport performance. On the other hand, due to the strong phonon interface scattering caused by the layered interface, the thermal conductivity of the polymer matrix is often low. It has been proved that the composite material containing GDY and PVDF shows high thermal conductivity for electronic cooling applications (Fig. 14a).<sup>164</sup> The Seebeck coefficient is enhanced in 2D materials because of the quantum confinement effect. The density of electron states near the Fermi level is efficiently enhanced, and a large number of net cross-sections in low-dimensional thermoelectric materials can effectively scatter phonons.<sup>166–168</sup> Especially, heteroatom doping can effectively regulate the energy band structure to optimize the thermoelectric properties. The concentration of intrinsic vacancies can also be

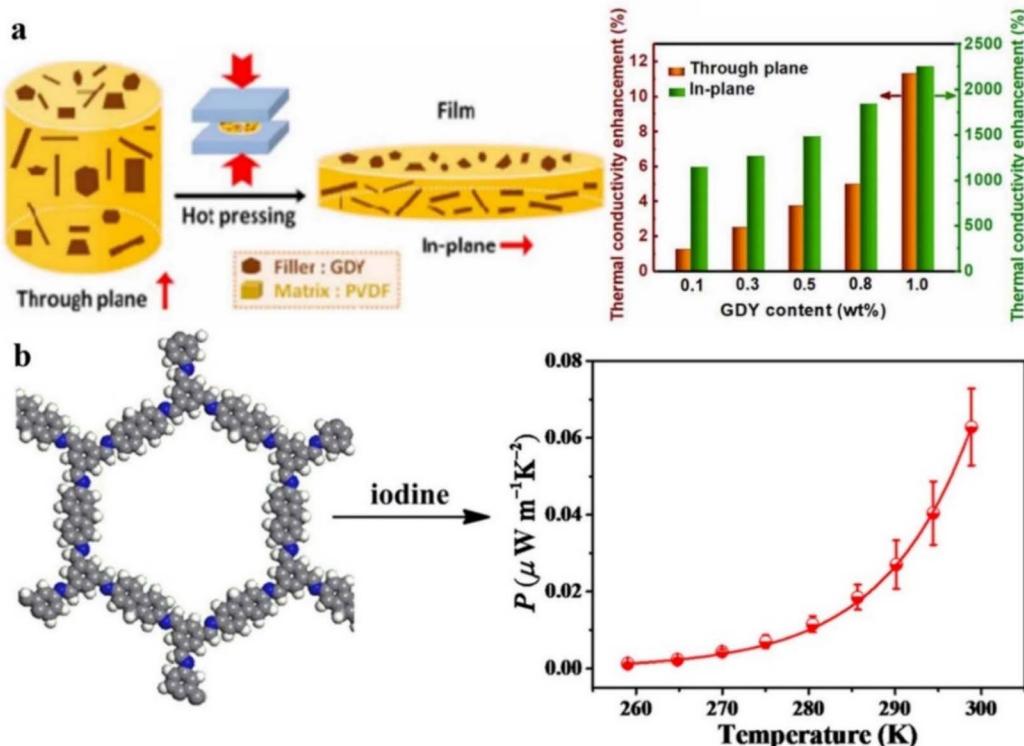


Fig. 14 (a) Synthesis and thermal transport properties of PVDF/GDY composite films. Adapted from ref. 164. Copyright 2022, Institute of Physics. (b) Iodine doped 2D COFs with improved thermoelectric properties. Adapted from ref. 165. Copyright 2017, American Chemical Society.

efficiently regulated. The Seebeck coefficient and power factor can be improved greatly because of doping iodine into COFs containing fluorene segments (Fig. 14b).<sup>165</sup> In addition, different preparation methods have great influence on the thermoelectric properties of materials.<sup>169</sup> Some new processes and methods of material synthesis are tried, and finally, electroacoustic decoupling regulation is achieved. For example, powder metallurgy methods can generally enhance phonon scattering and reduce lattice thermal conductivity through fine crystal processing.<sup>170</sup> Grain boundaries were reduced by the single crystal growth method, and the current carrier scattering mechanism was changed from ionization scattering to electro-acoustic scattering, which significantly improved the thermoelectric properties near room temperature.<sup>171</sup> With the continuous improvement of the performance of 2D materials in the field of thermoelectric devices, researchers have deeply explored the relationship between their structure and performance, understood the physical mechanism of electron-phonon transport, and explored innovative mechanisms and concepts of performance regulation, to further promote the application of high-efficiency thermoelectric devices based on 2D materials.<sup>172,173</sup>

### 3.3 Electrical and electrochemical properties

The regulation of the electronic structure and the manifestation of the intrinsic properties of 2D functional materials are inter-dependent. Particularly, the electrical and electrochemical properties of 2D materials can be greatly changed by adjusting the structure of the repeated units and the stacking mode between layers.<sup>18,81,91</sup> In addition, the stacking mode of 2D nanosheets also affects their band gap. For example, studies have shown that organic 2D materials can even exhibit metallic conductivity when the layers present a specific pattern of accumulation.<sup>174</sup> Functional 2D materials have great application prospects in electrochemical devices due to their electronic structure characteristics. Many research results also prove that the electrochemical devices prepared from 2D materials have good performance. Better device performance can be obtained by adjusting the structure morphology to suit the working principle and requirements of different electrochemical devices.<sup>176</sup> The performance in electrochemical devices can be optimized by changing the covalent bonding environment, or by introducing atomic-scale metal single atoms or nanoscale metal clusters through non-covalent bonding. For example, the special spherical structure of the material makes it easier to form a solid electrolyte interface film on the surface, thus greatly improving electrode stability and Coulomb efficiency.<sup>178</sup> On the other hand, the synergistic complexation of introduced heteroatoms with metal atoms induces strong electronic coupling and promotes the catalytically active site to carry out high-intensity charge transfer with the carrier, which is conducive to further improving the performance in electrochemical devices.<sup>54</sup> Recently, Li and co-workers have constructed a series of intelligent and multifunctional 2D GDY-based materials including smart ion channels using the concept of “ion channel self-expansion” to improve the charge

and discharge performance of lithium-ion batteries over a wide temperature range (Fig. 15a).<sup>77</sup> The proposed new mechanisms and concepts for the construction of multifunctional 2D materials can be used as key components for the self-power magnesium humidity battery. The exhibiting performance can be adjusted by external conditions such as humidity or sunlight, which can be regarded as a kind of intelligent electronic device (Fig. 15b).<sup>173</sup> On the other hand, the *in situ* fabrication of 2D materials with a hybrid structure can further optimize the physical and chemical properties of 2D functional GDY based materials. For instance, the hybrid structure of Zn atoms and GDY can effectively inhibit the formation of dendrites, thus greatly improving the life of the aqueous zinc ion batteries (Fig. 15c).<sup>174</sup> The stepwise induction of Zn atoms avoids the formation of dendrites. In another report, a heterogeneous hybrid structure containing  $\text{Cu}_{0.95}\text{V}_2\text{O}_5$  and GDY provides abundant Cu/O bivacancies, which was constructed by using self-catalytic GDY growth on copper containing metal oxides (Fig. 15d).<sup>175</sup> The strong interaction between metal ions and the alkyne bond makes the growth of GDY present a state of enyne complex in the inner layer and gradient GDY bond in the outer layer. The Cu and O vacancies enhance the ion transport kinetics of the  $\text{Cu}_{0.95}\text{V}_2\text{O}_5@\text{GDY}$  phase and increase the lithium storage sites. The material showed excellent fast charging performance and could be used as a cathode material to realize high-performance fast-charging lithium-ion batteries.

### 3.4 Optical-electrical transport properties

Because of the unique structure of 2D materials, many excellent properties different from those of three-dimensional bulk materials have been established in the aspect of the optical-electrical research field.<sup>59</sup> In particular, electrons and photons are not easily scattered during 2D lamellar transmission, which makes it have very unique transport properties in terms of electricity and optics. The conduction and valence bands of the 2D material can be tuned through structure decoration, intersecting at the point K in the Brillouin region around the Fermi level, forming a specific Dirac cone. In the vicinity of the Dirac cone, the energy and momentum of the electron have an adjustable relationship, showing semi-metallic characteristics.<sup>29,33,57,101</sup> A large number of studies have revealed that there are not only negatively charged electrons but also positively charged holes participating in the conductive process of functional 2D molecular structures consisting of organic segments.<sup>180–184</sup> The structural and chemical tunability and long-range crystal orderliness make 2D materials promising materials for a variety of applications, especially gas storage, separation, and catalysis. However, the inferior properties of most organic segments developed to date limit the use of these materials for applications requiring charge transfer over long distances. Thus, the recent discovery of conductive 2D materials opens another broad field for potential applications in the field of optoelectronics and chemical resistance sensing.<sup>185,186</sup> However, the mechanism of charge transport in semiconductor 2D materials remains unclear. Solving the fundamental principles of charge transport is critical to advancing the design



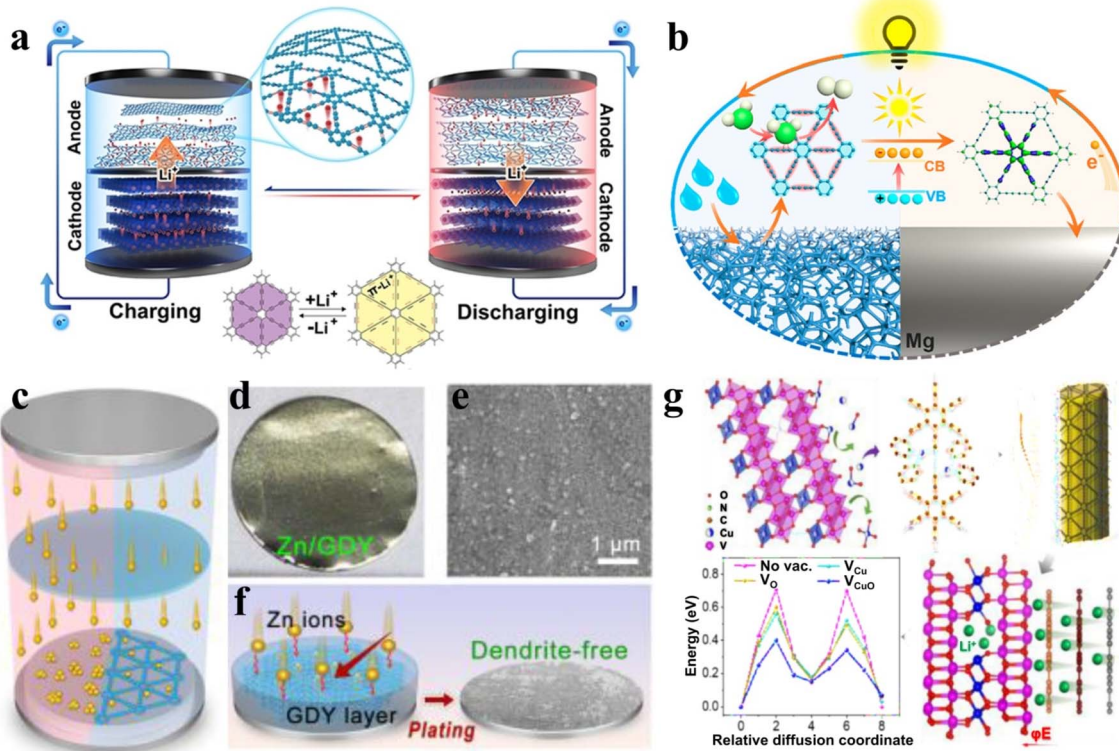
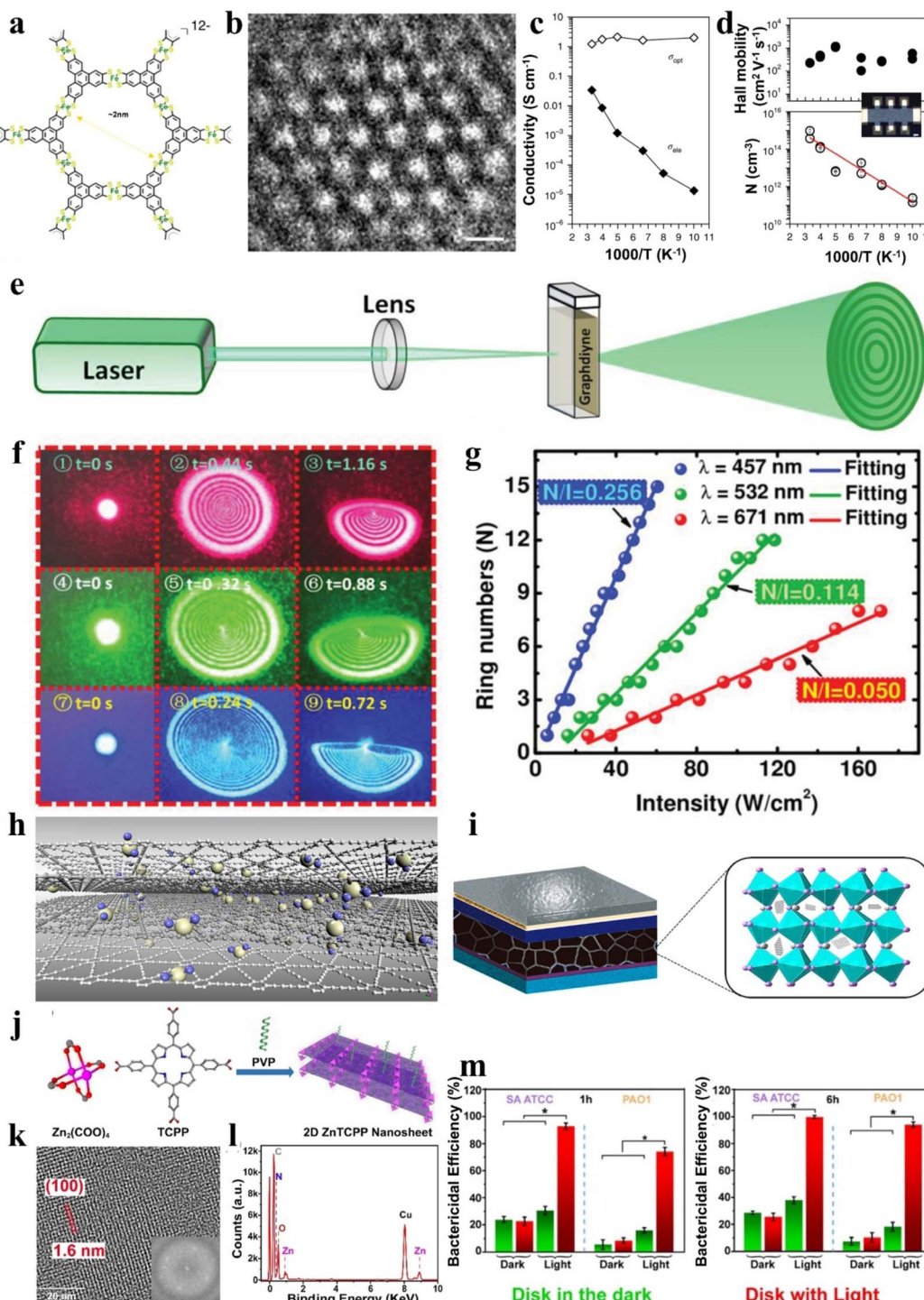


Fig. 15 Applications of 2D materials in energy storage batteries. (a) The self-expanding mechanism of GDY-based lithium-ion batteries. Adapted from ref. 77. (b) The GDY-based solid intelligent Mg-moisture battery with photoresponsivity and humidity responsive. Adapted from ref. 173. Copyright 2022, American Chemical Society. Copyright 2022, John Wiley & Sons. (c) and (f) The electroplating and assembly process of the Zn/GDY electrode. The picture (d) and SEM image (e) of Zn/GDY. Adapted from ref. 174. Copyright 2023, John Wiley & Sons. (g) Synthesis of Cu<sub>0.95</sub>V<sub>2</sub>O<sub>5</sub>@GDY and the mechanism of Cu<sub>0.95</sub>V<sub>2</sub>O<sub>5</sub>@GDY improving the performance of lithium-ion batteries. Adapted from ref. 175. Copyright 2022, John Wiley & Sons.

strategy and the application of such materials in optoelectronic applications. A novel  $\pi$ -d conjugated semiconducting two-dimensional MOF Fe<sub>3</sub>(THT)<sub>2</sub>(NH<sub>4</sub>)<sub>3</sub> has been prepared by an all-optical, contactless time-resolved Terahertz spectrum (TRTS) technique (Fig. 16a–d).<sup>177</sup> The room temperature mobility of the 2D semiconductor reaches 220 cm<sup>2</sup> V<sup>-1</sup> s<sup>-1</sup>. Ribbon transport in the porous 2D MOF is demonstrated. A direct infrared band gap of about 0.25 eV is observed. The structures of these 2D materials are highly controllable, so the authors expect that their conductivity, mobility, and band gap can be controlled with appropriate chemical design. From a synthesis perspective, developing single crystals and layering them into monolayers not only allows for fundamental research on structure–performance relationships but also enables the development of functional devices when long-distance free carrier motion is required.

2D materials have attracted more and more attention in the field of optical transport, photoelectric conversion, and photoelectric catalysis. Recent research also shows that 2D materials also have an ideal nonlinear response in visible light bands, which provides a strong guarantee for application in nonlinear optics. For example, by taking advantage of the strong nonlinear properties, researchers applied a 2D carbonic material to nonlinear photon diodes together with another back saturation

absorption material tin disulphide (SnS<sub>2</sub>).<sup>85</sup> The results show that the composite structure can realize the non-reciprocal propagation of light, so it can be used in the photon diode. In addition, a method to estimate the nonlinear refractive index of the composite structure is proposed by using the non-reciprocal propagation properties of the composite structure to light, namely the similarity contrast method. By comparison, the results show that the nonlinear refractive index can reach 10<sup>-5</sup> cm<sup>2</sup> W<sup>-1</sup> (Fig. 16e–g). The 2D layered structure shows strong light-matter forces and sufficient stability to achieve a wide-band optical response, contributing to the enhancement of the ability of light harvesting, which also demonstrates the potential of applications in optoelectronic (Fig. 16h–i)<sup>178</sup> and photocatalytic (Fig. 16j–m)<sup>179</sup> devices. A series of key properties of the active layer including domain sizes, grain boundaries, and crystalline qualities can be efficiently adjusted. The unique 2D structure restricts electrons to a 2D region, allowing them to move freely along the plane, making every active site on the surface available as a substrate for the reaction, without the diffusion restriction of molecules through the internal pores of the 3D material. The expanded surface area of 2D photocatalytic systems has great benefits for light collection, mass transport, and exposure to abundant surface-active sites. In addition, the ultra-thin properties of 2D materials significantly reduce the



**Fig. 16** Optical applications of 2D materials. (a) Structure and (b) HR-TEM of the  $\text{Fe}_3(\text{THT})_2(\text{NH}_4)_3$  2D MOF. (c) and (d) Effect of temperature on the photoconductivity of  $\text{Fe}_3(\text{THT})_2(\text{NH}_4)_3$ . Adapted from ref. 177. Copyright 2018, Springer Nature. (e) Spatial self-phase modulation (SSPM) experiment of GDY dispersions. (f) The diffraction rings obtained by the SSPM experiment. (g) The nonlinear optical response of GDY dispersions. Adapted from ref. 85. Copyright 2022, John Wiley & Sons. (h) Structure of the adduct between GDY and  $\text{PbI}_2$  of the perovskite solar cell. (i) Structure of the perovskite solar cell used GDY as a host material. Adapted from ref. 178. Copyright 2018, American Chemical Society. (j) Synthesis, (k) HR-TEM, and (l) EDX of heterogeneous photocatalysts ZnTCPP nanosheets. (m) Bactericidal activity of 3D printed disks containing ZnTCPP nanosheets. Adapted from ref. 179. Copyright 2021, John Wiley & Sons.

migration distance of charge from the body phase to the surface, improving charge separation. In short, compared with 3D materials, 2D materials' ultra-thin morphology can provide

many exposed active sites, which is conducive to the mass transfer and electron transfer process. The unsaturated coordination site is equivalent to the introduction of defects, which

greatly improves the efficiency of photoelectric conversion and the catalytic activity of photoelectric processes.<sup>24,33,135,164</sup>

### 3.5 Bio-activity

2D materials have unique properties such as a large specific surface area, superior optical, electrical, and electrochemical activity, which can satisfy the application requirements in the field of biomedicine, biosensing, and disease treatment.<sup>187-189</sup> In addition, the large structural variety of synthetic 2D materials provides abundant choices for various nano-biotic applications; the facile preparation process is easy for large-scale production.<sup>49</sup> At the same time, 2D materials can form different composites with various biomolecules through a self-assembly method, showing a good structure, function, and application prospects.<sup>190</sup> The above advantage in the structure and properties of 2D materials makes them widely studied. Some bottleneck problems in the related field can be solved.<sup>49</sup> For instance, the hematopoietic tumour is one of the most common malignant tumours and also an important disease affecting people's health, including leukaemia, lymphoma, myeloproliferative tumours, multiple myeloma, and so on.<sup>191</sup> Due to complex characterization and diverse classification, the characterization of haematological tumours is complex and difficult to treat. Most recently, Qian and co-workers have developed specific therapeutic strategies for different types of lymphoma cells (Fig. 17).<sup>190</sup> Lymphoma is a malignant tumour of the hematopoietic system. There are some problems in its clinical

treatment, such as poor efficacy and easy recurrence. Therefore, there is an urgent and unmet need to explore new treatments for lymphoma. B-cell lymphomas have immunosuppressive and inflammatory microenvironments, which makes treatment more difficult while interacting with tumour stem cells. GDYO, a 2D nanosheet with a size of 200–500 nm and a thickness of less than 1 nm, has a toxic effect on lymphoma. On the one hand, GDYO can directly kill tumour stem cells, and on the other hand, GDYO can reshape the lymphoma microenvironment and inhibit the growth of lymphoma, thus delivering a double blow to lymphoma. In addition, the experiment showed that GDYO treatment had no significant adverse effects on the hematopoietic system, various organs, and subsequent survival of mice. These results indicate that GDYO has high biosafety and biocompatibility while effectively treating lymphoma. GDYO is also expected to be a promising drug in the treatment of leukemia. The most frequently mutated gene in acute myeloid leukaemia (AML) is DNA methyltransferase 3A (DNMT3A). High cell adhesion of DNMT3A mutant AML leads to rapid disease deterioration, high recurrence rate, and poor prognosis in DNMT3A mutant AML patients. Wang *et al.* found that DNMT3A mutated AML cells were the major enrichment areas of cell adherence-related genes.<sup>191</sup> Under the action of the c-type mannose receptor (MRC2) and integrin  $\beta$ 2 (ITGB2), GDYO is effectively attached to the mutant cells and internalized. At the same time, GDYO binds to actin and prevents actin from aggregating. This damages the cell structure and eventually leads to cell decay. Glucose is an important basis for the

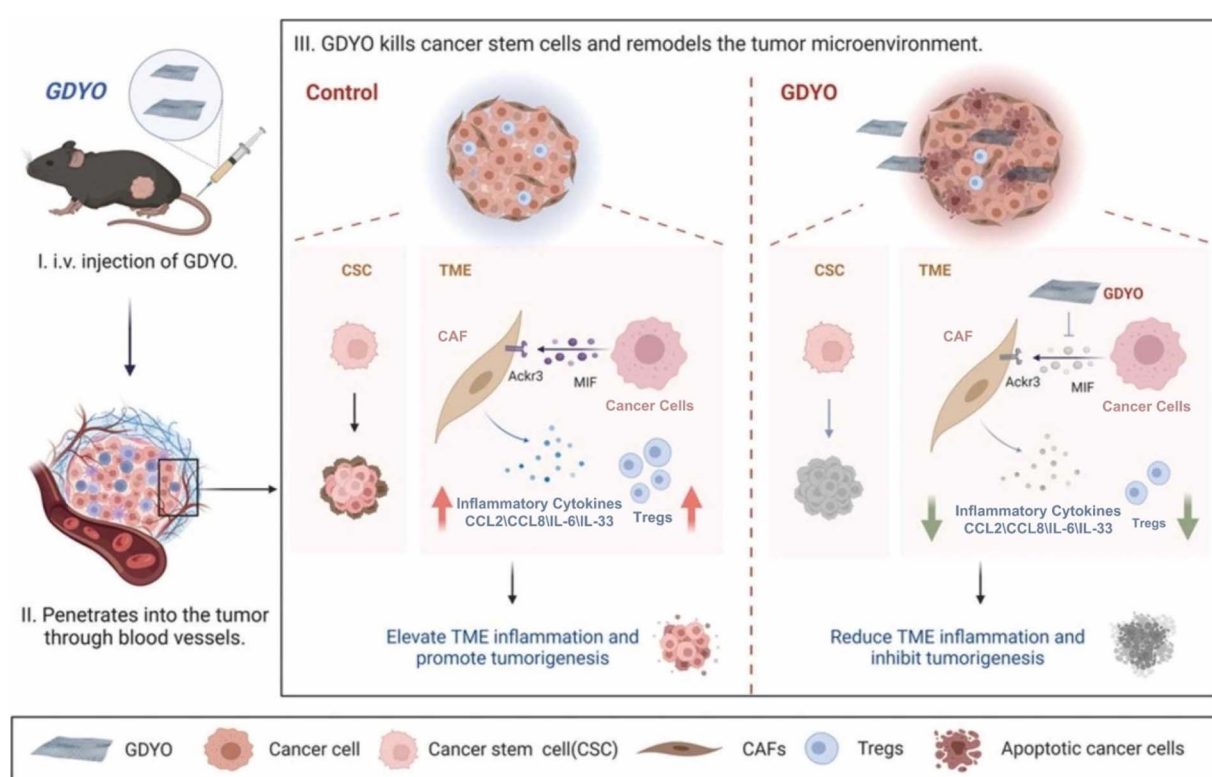


Fig. 17 Biological applications of 2D materials. The duplex anti-lymphoma effects of GDY oxide (GDYO). Adapted from ref. 190. Copyright 2022, Elsevier.



diagnosis of diabetes. The commonly used glucose detection method, glucose oxidase-peroxidase ( $GO_x$ -POD) method, has high sensitivity and a low detection limit. However, this method requires two separate reactions catalysed by different enzymes to complete the glucose detection. Liu *et al.* utilized the characteristics of GDY, such as a large specific surface area, sp<sup>2</sup> hybrid carbon atoms, and uneven energy distribution, to stabilize  $Fe^{2+}$  and glucose oxidase on GDY.<sup>192</sup> The complex has the activity of peroxidase and glucose oxidase at the same time, successfully realizing the one-step detection of glucose. This demonstrates the broad application prospect of 2D GDY in biosensing.

## 4. Conclusion and prospects

This review focuses on the recent advances in structural modification, self-assembly, basic properties, and related device applications of functional 2D materials. The preparation strategies are summarized and discussed from the following aspects. The structure and intrinsic properties of 2D materials can be effectively regulated by chemical structure decoration and preparation process control. The bonding direction of covalent bonds can be controlled by adjusting the chemical structure of the active linking groups. The diversity of non-covalent bonds in the aggregates of 2D materials determines the size and morphology of the prepared assemblies. Based on this, multifunctional 2D materials can be constructed and used as a cornerstone for subsequent orderly growth and self-assembly. The as-prepared 2D materials can be further functionalized through compositing with metal atoms or other components. The morphology and function of ordered self-assembly based on supramolecular interactions of related material systems have attracted extensive attention, which makes them exhibit unique mechanical, electrical, optical, and photoelectric properties, and are widely used in energy storage and conversion, catalysis, optoelectronics, and biosensors.

Although remarkable progress has been achieved, studies on functional 2D materials are still at their primary stage. Some fundamental scientific issues, especially on the structure–performance correlation, still need to be deeply understood. On the other hand, according to the development needs of different application fields, it is necessary to further improve the structure of 2D material systems, to optimize the performance of existing devices and expand their application fields. At present, the main challenges are as follows:

(1) In the aspect of synthesis, the method of interfacial growth has been extensively reported, and the reaction conditions should be controlled more accurately. The homogeneous growth based on the self-assembly of the precursor should be further explored and perfected, and irreversible reactions will show more and more advantages in the construction of rigid 2D materials. The rapid development of GDY-based materials prepared through the coupling between terminal acetylenic groups provides a comprehensive platform to systematically optimize the coupling conditions and investigate the reaction process. Besides that, some new fabrication strategies, such as “crystal-to-crystal” and “post-treated” strategies, should be

further developed to fabricate functional 2D materials with novel structures. Combining the theory analysis on the reaction process and experimental results on the *in situ* characterization is helpful to understand the preparation mechanism and construct the accurate structure model of functional 2D material system.

(2) It is necessary to develop a simple and convenient preparation method. It is an effective way to solve the problem to make full use of multi-scale compound effects from the micro- to the macro-scale. At present, most of the assembly systems based on 2D materials can only be carried out in a specific scale range, such as single micron, submicron, and nanoscale. Further development is similar to the natural assembly function with specific functions, to realize the multi-stage assembly of structural units of different scales, and combine the unique functions of different components, to develop the system of 2D materials with multi-scale and multi-component synergies. It is extremely crucial for the new-emerging functional 2D materials such as GDY, which possesses organized arrangement of functional segments including different hybridized types of carbon atoms, and different kinds of heteroatoms. It can be expected that while functional 2D materials achieve long-range order at the macro-scale, the designed structural advantages can be fully exhibited, which is the key common issue of the related research. For instance, achieving rapid preparation on a large scale by a simple method; accurately controlling the number of layers and morphology; controlling photoelectric properties effectively are still the key problems limiting the development and application of GDY-based materials.

(3) It is necessary to consider an environmentally friendly preparation route to prepare 2D materials. Some innovative coupling processes in a metal catalyst-free reaction system triggered by other mechanisms such as light, thermal, or microwaves need to be systematically considered.

(4) At present, understanding of the relationship between the structure of 2D materials and related electrical and optical intrinsic properties is still very limited. Further systematic theoretical research is needed to reveal the intrinsic relationship between materials and properties. The aggregation morphology and physicochemical properties of the current molecular system need to be further explored by combining theoretical experiments.

(5) In practical applications, some energy storage devices need to run repeatedly within a long cycle or operate under more severe conditions such as high or low temperature. Therefore, improving the chemical, mechanical, and thermal stability of 2D materials is very important for broadening the practical application. For instance, the stability of GDY-based materials can be effectively improved by coordinating metal with a high oxidation state, which inspires novel research ideas for other synthetic 2D functional materials.

Based on the above discussion, 2D materials show unique advantages of structural properties and development potential. The application of the new generation of 2D materials will have a bright prospect and bring about new vitality to the development and prosperity of materials science.



## Author contributions

L. W. Z. and N. W. conducted the literature research and drafted the manuscript. N. W. and Y. L. L. conceived the topic and structure of the article. Y. L. L. supervised the completion of the manuscript. All authors reviewed and contributed to this manuscript.

## Conflicts of interest

There are no conflicts of interest to declare.

## Acknowledgements

This work is supported by the National Natural Science Foundation of China (22275115), National Key Research and Development Project of China (2018YFA0703501), and Young Scholarship Funding of Shandong University.

## References

- 1 B. Kahr and M. D. Ward, *Nat. Chem.*, 2017, **10**, 4–6.
- 2 M. W. Terban and S. J. L. Billinge, *Chem. Rev.*, 2022, **122**, 1208–1272.
- 3 G. Zhang, B. Hua, A. Dey, M. Ghosh, B. A. Moosa and N. M. Khashab, *Acc. Chem. Res.*, 2021, **54**, 155–168.
- 4 Y. B. Zhao, V. Wang and A. Javey, *Matter*, 2020, **3**, 1832–1844.
- 5 P. H. Li, M. R. Ryder and J. F. Stoddart, *Acc. Mater. Res.*, 2020, **1**, 77–87.
- 6 Z. Q. Zheng, Y. R. Xue and Y. L. Li, *Trends Chem.*, 2022, **4**, 754–768.
- 7 H. Yu, Y. Xue and Y. Li, *Adv. Mater.*, 2019, **31**, e1803101.
- 8 W. Li, H. Ma, S. Li and J. Ma, *Chem. Sci.*, 2021, **12**, 14987–15006.
- 9 D. B. Amabilino, D. K. Smith and J. W. Steed, *Chem. Soc. Rev.*, 2017, **46**, 2404–2420.
- 10 C. Y. Xu, Z. J. Zhao, K. X. Yang, L. B. Niu, X. L. Ma, Z. J. Zhou, X. L. Zhang and F. J. Zhang, *J. Mater. Chem. A*, 2022, **10**, 6291–6329.
- 11 O. Sato, *Nat. Chem.*, 2016, **8**, 644–656.
- 12 Y. S. Zhao, N. L. Yang, C. D. Wang, L. Song, R. B. Yu and D. Wang, *APL Mater.*, 2021, **9**, 071102.
- 13 B. K. Liu, L. K. Xu, Y. S. Zhao, J. Du, N. L. Yang and D. Wang, *J. Mater. Chem. A*, 2021, **9**, 19298–19316.
- 14 S. H. Zhan, X. B. Chen, B. Xu, L. Wang, L. M. Tong, R. B. Yu, N. L. Yang and D. Wang, *Nano Today*, 2022, **47**, 101626.
- 15 B. Liu, S. Zhan, J. Du, X. Yang, Y. Zhao, L. Li, J. Wan, Z. J. Zhao, J. Gong, N. Yang, R. Yu and D. Wang, *Adv. Mater.*, 2022, e2206450, DOI: [10.1002/adma.202206450](https://doi.org/10.1002/adma.202206450).
- 16 Y. Zhao, J. Wan, N. Yang, R. Yu and D. Wang, *Mater. Chem. Front.*, 2021, **5**, 7987–7992.
- 17 Y. Zhao, N. Yang, H. Yao, D. Liu, L. Song, J. Zhu, S. Li, L. Gu, K. Lin and D. Wang, *J. Am. Chem. Soc.*, 2019, **141**, 7240–7244.
- 18 Y. Zhao, N. L. Yang, R. B. Yu, Y. Zhang, J. Zhang, Y. L. Li and D. Wang, *Energychem*, 2020, **2**, 100041.
- 19 J. Long, M. S. Ivanov, V. A. Khomchenko, E. Mamontova, J. M. Thibaudeau, J. Rouquette, M. Beaudhuin, D. Granier, R. A. S. Ferreira, L. D. Carlos, B. Donnadieu, M. S. C. Henriques, J. A. Paixao, Y. Guari and J. Larionova, *Science*, 2020, **367**, 671–676.
- 20 D. P. August, R. A. W. Dryfe, S. J. Haigh, P. R. C. Kent, D. A. Leigh, J. F. Lemonnier, Z. Li, C. A. Muryn, L. I. Palmer, Y. Song, G. F. S. Whitehead and R. J. Young, *Nature*, 2020, **588**, 429–435.
- 21 N. T. Yao, L. Zhao, H. Y. Sun, C. Yi, Y. H. Guan, Y. M. Li, H. Oshio, Y. S. Meng and T. Liu, *Angew. Chem., Int. Ed.*, 2022, **61**, e202208208.
- 22 B. Ma, G. Chen, C. Fave, L. Chen, R. Kuriki, K. Maeda, O. Ishitani, T. C. Lau, J. Bonin and M. Robert, *J. Am. Chem. Soc.*, 2020, **142**, 6188–6195.
- 23 Z. Jia, Y. Li, Z. Zuo, H. Liu, C. Huang and Y. Li, *Acc. Chem. Res.*, 2017, **50**, 2470–2478.
- 24 L. J. Du, T. Hasan, A. Castellanos-Gomez, G. B. Liu, Y. G. Yao, C. N. Lau and Z. P. Sun, *Nat. Rev. Phys.*, 2021, **3**, 193–206.
- 25 D. Rhodes, S. H. Chae, R. Ribeiro-Palau and J. Hone, *Nat. Mater.*, 2019, **18**, 541–549.
- 26 H. Li, S. Ruan and Y. J. Zeng, *Adv. Mater.*, 2019, **31**, e1900065.
- 27 R. Frisenda, E. Navarro-Moratalla, P. Gant, D. Perez De Lara, P. Jarillo-Herrero, R. V. Gorbachev and A. Castellanos-Gomez, *Chem. Soc. Rev.*, 2018, **47**, 53–68.
- 28 D. Geng and H. Y. Yang, *Adv. Mater.*, 2018, **30**, e1800865.
- 29 G. Chakraborty, I. H. Park, R. Medishetty and J. J. Vittal, *Chem. Rev.*, 2021, **121**, 3751–3891.
- 30 D. Cui, D. F. Perepichka, J. M. MacLeod and F. Rosei, *Chem. Soc. Rev.*, 2020, **49**, 2020–2038.
- 31 Y. Huang, J. Liang, C. Wang, S. Yin, W. Fu, H. Zhu and C. Wan, *Chem. Soc. Rev.*, 2020, **49**, 6866–6883.
- 32 C. L. Ye, D. Q. Chao, J. Shan, H. Li, K. Davey and S. Z. Qiao, *Matter*, 2020, **2**, 323–344.
- 33 N. R. Glavin, R. Rao, V. Varshney, E. Bianco, A. Apte, A. Roy, E. Ringe and P. M. Ajayan, *Adv. Mater.*, 2020, **32**, e1904302.
- 34 M. Gibertini, M. Koperski, A. F. Morpurgo and K. S. Novoselov, *Nat. Nanotechnol.*, 2019, **14**, 408–419.
- 35 S. Das, D. Pandey, J. Thomas and T. Roy, *Adv. Mater.*, 2019, **31**, e1802722.
- 36 S. Bertolazzi, P. Bondavalli, S. Roche, T. San, S. Y. Choi, L. Colombo, F. Bonaccorso and P. Samori, *Adv. Mater.*, 2019, **31**, e1806663.
- 37 X. Xiao, H. Wang, P. Urbankowski and Y. Gogotsi, *Chem. Soc. Rev.*, 2018, **47**, 8744–8765.
- 38 Y. Fang, Y. R. Xue, L. Hui, H. D. Yu and Y. L. Li, *Angew. Chem., Int. Ed.*, 2021, **60**, 3170–3174.
- 39 A. Govind Rajan, K. S. Silmore, J. Swett, A. W. Robertson, J. H. Warner, D. Blankschtein and M. S. Strano, *Nat. Mater.*, 2019, **18**, 129–135.
- 40 L. Li, Q. Yun, C. Zhu, G. Sheng, J. Guo, B. Chen, M. Zhao, Z. Zhang, Z. Lai, X. Zhang, Y. Peng, Y. Zhu and H. Zhang, *J. Am. Chem. Soc.*, 2022, **144**, 6475–6482.



41 V. A. Kuehl, J. Yin, P. H. H. Duong, B. Mastorovich, B. Newell, K. D. Li-Oakey, B. A. Parkinson and J. O. Hoberg, *J. Am. Chem. Soc.*, 2018, **140**, 18200–18207.

42 Z. Shuhui, Z. Yasong, Y. Nailiang and W. Dan, *Chem. J. Chin. Univ.*, 2021, **42**, 333–348.

43 Y. Wang, H. Liu, Q. Pan, C. Wu, W. Hao, J. Xu, R. Chen, J. Liu, Z. Li and Y. Zhao, *J. Am. Chem. Soc.*, 2020, **142**, 5958–5963.

44 L. Grill and S. Hecht, *Nat. Chem.*, 2020, **12**, 115–130.

45 L. Cao, X. Liu, D. B. Shinde, C. Chen, I. C. Chen, Z. Li, Z. Zhou, Z. Yang, Y. Han and Z. Lai, *Angew. Chem., Int. Ed.*, 2022, **61**, e202113141.

46 M. Pfeffermann, R. Dong, R. Graf, W. Zajaczkowski, T. Gorelik, W. Pisula, A. Narita, K. Mullen and X. Feng, *J. Am. Chem. Soc.*, 2015, **137**, 14525–14532.

47 Y. Peng, L. Li, C. Zhu, B. Chen, M. Zhao, Z. Zhang, Z. Lai, X. Zhang, C. Tan, Y. Han, Y. Zhu and H. Zhang, *J. Am. Chem. Soc.*, 2020, **142**, 13162–13169.

48 I. Hisaki, C. Xin, K. Takahashi and T. Nakamura, *Angew. Chem., Int. Ed.*, 2019, **58**, 11160–11170.

49 T. Kim, J. Y. Park, J. Hwang, G. Seo and Y. Kim, *Adv. Mater.*, 2020, **32**, e2002405.

50 J. Wang, N. Li, Y. Xu and H. Pang, *Chemistry*, 2020, **26**, 6402–6422.

51 M. Wang, R. Dong and X. Feng, *Chem. Soc. Rev.*, 2021, **50**, 2764–2793.

52 H. Zhong, M. Wang, G. Chen, R. Dong and X. Feng, *ACS Nano*, 2022, **16**, 1759–1780.

53 Z. Yuan, X. Xiao, J. Li, Z. Zhao, D. Yu and Q. Li, *Adv. Sci.*, 2018, **5**, 1700626.

54 Y. Xue, B. Huang, Y. Yi, Y. Guo, Z. Zuo, Y. Li, Z. Jia, H. Liu and Y. Li, *Nat. Commun.*, 2018, **9**, 1460.

55 H. Sahabudeen, H. Qi, B. A. Glatz, D. Tranca, R. Dong, Y. Hou, T. Zhang, C. Kuttner, T. Lehnert, G. Seifert, U. Kaiser, A. Fery, Z. Zheng and X. Feng, *Nat. Commun.*, 2016, **7**, 13461.

56 Z. Dai, L. Liu and Z. Zhang, *Adv. Mater.*, 2019, **31**, e1805417.

57 X. Liu, S. M. Cho, S. Lin, Z. Chen, W. Choi, Y.-M. Kim, E. Yun, E. H. Baek, D. H. Ryu and H. Lee, *Matter*, 2022, **5**, 2306–2318.

58 J. Sun, Y. Choi, Y. J. Choi, S. Kim, J. H. Park, S. Lee and J. H. Cho, *Adv. Mater.*, 2019, **31**, e1803831.

59 F. Yang, S. Cheng, X. Zhang, X. Ren, R. Li, H. Dong and W. Hu, *Adv. Mater.*, 2018, **30**, 1702415.

60 S. M. Akkanen, H. A. Fernandez and Z. Sun, *Adv. Mater.*, 2022, **34**, e2110152.

61 Y. Zhao, H. Liu, C. Wu, Z. Zhang, Q. Pan, F. Hu, R. Wang, P. Li, X. Huang and Z. Li, *Angew. Chem., Int. Ed.*, 2019, **58**, 5376–5381.

62 F. Hu, W. Hao, D. Mucke, Q. Pan, Z. Li, H. Qi and Y. Zhao, *J. Am. Chem. Soc.*, 2021, **143**, 5636–5642.

63 Y. Zeng, P. Gordiichuk, T. Ichihara, G. Zhang, E. Sandoz-Rosado, E. D. Wetzel, J. Tresback, J. Yang, D. Kozawa, Z. Yang, M. Kuehne, M. Quien, Z. Yuan, X. Gong, G. He, D. J. Lundberg, P. Liu, A. T. Liu, J. F. Yang, H. J. Kulik and M. S. Strano, *Nature*, 2022, **602**, 91–95.

64 R. Matsuoka, R. Sakamoto, K. Hoshiko, S. Sasaki, H. Masunaga, K. Nagashio and H. Nishihara, *J. Am. Chem. Soc.*, 2017, **139**, 3145–3152.

65 J. Huang, Y. Li, R. K. Huang, C. T. He, L. Gong, Q. Hu, L. Wang, Y. T. Xu, X. Y. Tian, S. Y. Liu, Z. M. Ye, F. Wang, D. D. Zhou, W. X. Zhang and J. P. Zhang, *Angew. Chem., Int. Ed.*, 2018, **57**, 4632–4636.

66 L. Hui, X. Zhang, Y. Xue, X. Chen, Y. Fang, C. Xing, Y. Liu, X. Zheng, Y. Du, C. Zhang, F. He and Y. Li, *J. Am. Chem. Soc.*, 2022, **144**, 1921–1928.

67 J. T. Kim, C. W. Lee, H. J. Jung, H. J. Choi, A. Salman, S. Padmajan Sasikala and S. O. Kim, *ACS Nano*, 2022, **16**, 17687–17707.

68 V. Orts Mercadillo, K. C. Chan, M. Caironi, A. Athanassiou, I. A. Kinloch, M. Bissett and P. Cataldi, *Adv. Funct. Mater.*, 2022, **32**, 2204772.

69 S. Liu, J. Wang, J. Shao, D. Ouyang, W. Zhang, S. Liu, Y. Li and T. Zhai, *Adv. Mater.*, 2022, **34**, e2200734.

70 X. Xu, T. Guo, H. Kim, M. K. Hota, R. S. Alsaadi, M. Lanza, X. Zhang and H. N. Alshareef, *Adv. Mater.*, 2022, **34**, e2108258.

71 W. R. Zheng and L. Y. S. Lee, *Matter*, 2022, **5**, 515–545.

72 X. C. Zheng, Y. R. Xue, C. Zhang and Y. L. Li, *CCS Chem.*, 2022, DOI: [10.31635/ccschem.022.202202189](https://doi.org/10.31635/ccschem.022.202202189).

73 Y. X. Liu, Y. Gao, F. He, Y. R. Xue and Y. L. Li, *CCS Chem.*, 2023, **5**, 971–981.

74 F. He and Y. L. Li, *CCS Chem.*, 2023, **5**, 72–94.

75 Y. Gao, Y. Xue, L. Qi, C. Xing, X. Zheng, F. He and Y. Li, *Nat. Commun.*, 2022, **13**, 5227.

76 Y. Gao, Y. Xue, F. He and Y. Li, *Proc. Natl. Acad. Sci. U. S. A.*, 2022, **119**, e2206946119.

77 J. An, H. Zhang, L. Qi, G. Li and Y. Li, *Angew. Chem., Int. Ed.*, 2022, **61**, e202113313.

78 H. Yu, Y. Xue, L. Hui, C. Zhang, Y. Fang, Y. Liu, X. Chen, D. Zhang, B. Huang and Y. Li, *Natl. Sci. Rev.*, 2021, **8**, nwaa213.

79 Z. Zuo, F. He, F. Wang, L. Li and Y. Li, *Adv. Mater.*, 2020, **32**, e2004379.

80 C. Xing, Y. Xue, B. Huang, H. Yu, L. Hui, Y. Fang, Y. Liu, Y. Zhao, Z. Li and Y. Li, *Angew. Chem., Int. Ed.*, 2019, **58**, 13897–13903.

81 F. Wang, Z. Zuo, L. Li, F. He, F. Lu and Y. Li, *Adv. Mater.*, 2019, **31**, e1806272.

82 L. Hui, Y. Xue, H. Yu, Y. Liu, Y. Fang, C. Xing, B. Huang and Y. Li, *J. Am. Chem. Soc.*, 2019, **141**, 10677–10683.

83 L. Hui, Y. Xue, B. Huang, H. Yu, C. Zhang, D. Zhang, D. Jia, Y. Zhao, Y. Li, H. Liu and Y. Li, *Nat. Commun.*, 2018, **9**, 5309.

84 C. Lu, Y. Yang, J. Wang, R. Fu, X. Zhao, L. Zhao, Y. Ming, Y. Hu, H. Lin, X. Tao, Y. Li and W. Chen, *Nat. Commun.*, 2018, **9**, 752.

85 L. Wu, Y. Dong, J. Zhao, D. Ma, W. Huang, Y. Zhang, Y. Wang, X. Jiang, Y. Xiang, J. Li, Y. Feng, J. Xu and H. Zhang, *Adv. Mater.*, 2019, **31**, e1807981.

86 K. S. Novoselov, A. K. Geim, S. V. Morozov, D. Jiang, M. I. Katsnelson, I. V. Grigorieva, S. V. Dubonos and A. A. Firsov, *Nature*, 2005, **438**, 197–200.



87 K. S. Novoselov, A. K. Geim, S. V. Morozov, D. Jiang, Y. Zhang, S. V. Dubonos, I. V. Grigorieva and A. A. Firsov, *Science*, 2004, **306**, 666–669.

88 Y. S. Zhao, L. J. Zhang, J. Qi, Q. Jin, K. F. Lin and D. Wang, *Acta Phys.-Chim. Sin.*, 2018, **34**, 1048–1060.

89 D. Rodriguez-San-Miguel, C. Montoro and F. Zamora, *Chem. Soc. Rev.*, 2020, **49**, 2291–2302.

90 C. Huang, Y. Li, N. Wang, Y. Xue, Z. Zuo, H. Liu and Y. Li, *Chem. Rev.*, 2018, **118**, 7744–7803.

91 H. Shen, Y. J. Li and Y. L. Li, *Aggregate*, 2020, **1**, 57–68.

92 Y. Fang, Y. Liu, L. Qi, Y. Xue and Y. Li, *Chem. Soc. Rev.*, 2022, **51**, 2681–2709.

93 C. S. Huang, S. L. Zhang, H. B. Liu, Y. J. Li, G. T. Cui and Y. L. Li, *Nano Energy*, 2015, **11**, 481–489.

94 W. Zhou, H. Shen, C. Wu, Z. Tu, F. He, Y. Gu, Y. Xue, Y. Zhao, Y. Yi, Y. Li and Y. Li, *J. Am. Chem. Soc.*, 2019, **141**, 48–52.

95 H. Shang, Z. Zuo, L. Li, F. Wang, H. Liu, Y. Li and Y. Li, *Angew. Chem., Int. Ed.*, 2018, **57**, 774–778.

96 J. Li, Y. Yi, X. Zuo, B. Hu, Z. Xiao, R. Lian, Y. Kong, L. Tong, R. Shao, J. Sun and J. Zhang, *ACS Nano*, 2022, **16**, 3163–3172.

97 I. Insua, J. Bergueiro, A. Mendez-Ardoy, I. Lostale-Seijo and J. Montenegro, *Chem. Sci.*, 2022, **13**, 3057–3068.

98 Y. Li, L. Xu, H. Liu and Y. Li, *Chem. Soc. Rev.*, 2014, **43**, 2572–2586.

99 G. Li, Y. Li, H. Liu, Y. Guo, Y. Li and D. Zhu, *Chem. Commun.*, 2010, **46**, 3256–3258.

100 Z. Q. Zheng, L. Qi, Y. R. Xue and Y. L. Li, *Nano Today*, 2022, **43**, 101431.

101 H. Y. Zhu, X. Gan, A. McCreary, R. T. Lv, Z. Lin and M. Terrones, *Nano Today*, 2020, **30**, 100829.

102 N. Wang, J. He, Z. Tu, Z. Yang, F. Zhao, X. Li, C. Huang, K. Wang, T. Jiu, Y. Yi and Y. Li, *Angew. Chem., Int. Ed.*, 2017, **56**, 10740–10745.

103 J. J. He, N. Wang, Z. Yang, X. Y. Shen, K. Wang, C. S. Huang, Y. P. Yi, Z. Y. Tu and Y. L. Li, *Energy Environ. Sci.*, 2018, **11**, 2893–2903.

104 J. He, N. Wang, Z. Cui, H. Du, L. Fu, C. Huang, Z. Yang, X. Shen, Y. Yi, Z. Tu and Y. Li, *Nat. Commun.*, 2017, **8**, 1172.

105 Y. R. Xue, Y. L. Li, J. Zhang, Z. F. Liu and Y. L. Zhao, *Sci. China Chem.*, 2018, **61**, 765–786.

106 Y. Wang, J. An, L. Qi, Y. Xue, G. Li, Q. Lyu, W. Yang and Y. Li, *J. Am. Chem. Soc.*, 2023, **145**, 864–872.

107 C. Yin, J. Q. Li, T. R. Li, Y. Yu, Y. Kong, P. Gao, H. L. Peng, L. M. Tong and J. Zhang, *Adv. Funct. Mater.*, 2020, **30**, 2001396.

108 A. J. Mannix, Z. Zhang, N. P. Guisinger, B. I. Yakobson and M. C. Hersam, *Nat. Nanotechnol.*, 2018, **13**, 444–450.

109 R. Dong, T. Zhang and X. Feng, *Chem. Rev.*, 2018, **118**, 6189–6235.

110 R. Dong, M. Pfeffermann, H. Liang, Z. Zheng, X. Zhu, J. Zhang and X. Feng, *Angew. Chem., Int. Ed.*, 2015, **54**, 12058–12063.

111 W. Dai, F. Shao, J. Szczerbinski, R. McCaffrey, R. Zenobi, Y. Jin, A. D. Schluter and W. Zhang, *Angew. Chem., Int. Ed.*, 2016, **55**, 213–217.

112 T. Bauer, Z. Zheng, A. Renn, R. Enning, A. Stemmer, J. Sakamoto and A. D. Schluter, *Angew. Chem., Int. Ed.*, 2011, **50**, 7879–7884.

113 W. Ran, A. Walz, K. Stoiber, P. Knecht, H. Xu, A. C. Papageorgiou, A. Huettig, D. Cortizo-Lacalle, J. P. Mora-Fuentes, A. Mateo-Alonso, H. Schlichting, J. Reichert and J. V. Barth, *Angew. Chem., Int. Ed.*, 2022, **61**, e202111816.

114 M. Liu, S. Li, J. Zhou, Z. Zha, J. Pan, X. Li, J. Zhang, Z. Liu, Y. Li and X. Qiu, *ACS Nano*, 2018, **12**, 12612–12618.

115 B. B. Dan and K. N. Shands, *Can. Med. Assoc. J.*, 1982, **126**, 751–752.

116 H. Liu, X. N. Kan, C. Y. Wu, Q. Y. Pan, Z. B. Li and Y. J. Zhao, *Chin. J. Polym. Sci.*, 2018, **36**, 425–444.

117 D. Zhou, X. Tan, H. Wu, L. Tian and M. Li, *Angew. Chem., Int. Ed.*, 2019, **58**, 1376–1381.

118 M. Wang, X. Dong, Z. Meng, Z. Hu, Y. G. Lin, C. K. Peng, H. Wang, C. W. Pao, S. Ding, Y. Li, Q. Shao and X. Huang, *Angew. Chem., Int. Ed.*, 2021, **60**, 11190–11195.

119 Y. Kong, X. Li, L. Wang, Z. Zhang, X. Feng, J. Liu, C. Chen, L. Tong and J. Zhang, *ACS Nano*, 2022, **16**, 11338–11345.

120 Z. Wang, Z. Zhang, H. Qi, A. Ortega-Guerrero, L. Wang, K. Xu, M. Wang, S. Park, F. Hennersdorf, A. Dianat, A. Croy, H. Komber, G. Cuniberti, J. J. Weigand, U. Kaiser, R. Dong and X. Feng, *Nat. Synth.*, 2021, **1**, 69–76.

121 X. Gao, Y. Zhu, D. Yi, J. Zhou, S. Zhang, C. Yin, F. Ding, S. Zhang, X. Yi, J. Wang, L. Tong, Y. Han, Z. Liu and J. Zhang, *Sci. Adv.*, 2018, **4**, eaat6378.

122 Y. Z. Yang, C. Schafer and K. Borjesson, *Chem.*, 2022, **8**, 2217–2227.

123 X. Kan, Y. Ban, C. Wu, Q. Pan, H. Liu, J. Song, Z. Zuo, Z. Li and Y. Zhao, *ACS Appl. Mater. Interfaces*, 2018, **10**, 53–58.

124 K. Park, H. Kang, S. Koo, D. Lee and S. Ryu, *Nat. Commun.*, 2019, **10**, 4931.

125 X. Kan, D. Wang, Q. Pan, Y. Wang, Y. Xiao, J. Liu, Y. Zhao and Z. Li, *Chemistry*, 2020, **26**, 7801–7807.

126 A. A. Vavilova, P. L. Padnya, T. A. Mukhametzyanov, A. V. Buzyurov, K. S. Usachev, D. R. Islamov, M. A. Ziganshin, A. E. Boldyrev and I. I. Stoikov, *Nanomaterials*, 2020, **10**, 2505.

127 Y. Wang, W. Hao, H. Liu, R. Chen, Q. Pan, Z. Li and Y. Zhao, *Nat. Commun.*, 2022, **13**, 100.

128 W. Liu, X. Li, C. Wang, H. Pan, W. Liu, K. Wang, Q. Zeng, R. Wang and J. Jiang, *J. Am. Chem. Soc.*, 2019, **141**, 17431–17440.

129 Q. H. Guo, M. Jia, Z. Liu, Y. Qiu, H. Chen, D. Shen, X. Zhang, Q. Tu, M. R. Ryder, H. Chen, P. Li, Y. Xu, P. Li, Z. Chen, G. S. Shekhawat, V. P. Dravid, R. Q. Snurr, D. Philp, A. C. Sue, O. K. Farha, M. Rolandi and J. F. Stoddart, *J. Am. Chem. Soc.*, 2020, **142**, 6180–6187.

130 B. J. Smith and W. R. Dichtel, *J. Am. Chem. Soc.*, 2014, **136**, 8783–8789.

131 Z. Zhao, R. Wang, C. Peng, W. Chen, T. Wu, B. Hu, W. Weng, Y. Yao, J. Zeng, Z. Chen, P. Liu, Y. Liu, G. Li, J. Guo, H. Lu and Z. Guo, *Nat. Commun.*, 2021, **12**, 6606.



132 S. Bi, C. Yang, W. Zhang, J. Xu, L. Liu, D. Wu, X. Wang, Y. Han, Q. Liang and F. Zhang, *Nat. Commun.*, 2019, **10**, 2467.

133 B. Han, X. Ding, B. Yu, H. Wu, W. Zhou, W. Liu, C. Wei, B. Chen, D. Qi, H. Wang, K. Wang, Y. Chen, B. Chen and J. Jiang, *J. Am. Chem. Soc.*, 2021, **143**, 7104–7113.

134 Y. Kong, J. Q. Li, S. Zeng, C. Yin, L. M. Tong and J. Zhang, *Chem.*, 2020, **6**, 1933–1951.

135 J. Li, S. Li, Q. Liu, C. Yin, L. Tong, C. Chen and J. Zhang, *Small*, 2019, **15**, e1805344.

136 H. Liu, J. Xu, Y. Li and Y. Li, *Acc. Chem. Res.*, 2010, **43**, 1496–1508.

137 Y. Zhao, J. Wan, H. Yao, L. Zhang, K. Lin, L. Wang, N. Yang, D. Liu, L. Song, J. Zhu, L. Gu, L. Liu, H. Zhao, Y. Li and D. Wang, *Nat. Chem.*, 2018, **10**, 924–931.

138 X. Z. Song, S. Y. Song, S. N. Zhao, Z. M. Hao, M. Zhu, X. Meng, L. L. Wu and H. J. Zhang, *Adv. Funct. Mater.*, 2014, **24**, 4034–4041.

139 X. Li, H. Xu, F. Kong and R. Wang, *Angew. Chem., Int. Ed.*, 2013, **52**, 13769–13773.

140 H. Ito, M. Muromoto, S. Kurenuma, S. Ishizaka, N. Kitamura, H. Sato and T. Seki, *Nat. Commun.*, 2013, **4**, 2009.

141 N. Y. Li, X. Y. Guo, L. L. Liu, J. Ma and D. Liu, *Dalton Trans.*, 2022, **51**, 17235–17240.

142 S. L. Huang, T. S. A. Hor and G. X. Jin, *Coord. Chem. Rev.*, 2017, **346**, 112–122.

143 R. Bhola, P. Payamyar, D. J. Murray, B. Kumar, A. J. Teator, M. U. Schmidt, S. M. Hammer, A. Saha, J. Sakamoto, A. D. Schluter and B. T. King, *J. Am. Chem. Soc.*, 2013, **135**, 14134–14141.

144 P. Kissel, D. J. Murray, W. J. Wulf Lange, V. J. Catalano and B. T. King, *Nat. Chem.*, 2014, **6**, 774–778.

145 B. Zhang, T. Fan, N. Xie, G. Nie and H. Zhang, *Adv. Sci.*, 2019, **6**, 1901787.

146 Y. Du, W. Zhou, J. Gao, X. Pan and Y. Li, *Acc. Chem. Res.*, 2020, **53**, 459–469.

147 Z. Zheng, F. He, Y. Xue and Y. Li, *Chem. Res. Chin. Univ.*, 2021, **38**, 92–98.

148 S. S. Zhang, Y. J. Cai, H. Y. He, Y. Q. Zhang, R. J. Liu, H. B. Cao, M. Wang, J. J. Liu, G. J. Zhang, Y. L. Li, H. B. Liu and B. Li, *J. Mater. Chem. A*, 2016, **4**, 4738–4744.

149 C. Xie, X. Hu, Z. Guan, X. Li, F. Zhao, Y. Song, Y. Li, X. Li, N. Wang and C. Huang, *Angew. Chem., Int. Ed.*, 2020, **59**, 13542–13546.

150 N. Wang, X. Li, Z. Tu, F. Zhao, J. He, Z. Guan, C. Huang, Y. Yi and Y. Li, *Angew. Chem., Int. Ed.*, 2018, **57**, 3968–3973.

151 N. Wang, J. He, K. Wang, Y. Zhao, T. Jiu, C. Huang and Y. Li, *Adv. Mater.*, 2019, **31**, e1803202.

152 Y. Peng, B. Lu and S. Chen, *Adv. Mater.*, 2018, **30**, e1801995.

153 Q. Qi, L. K. Xu, J. Du, N. L. Yang and D. Wang, *Chem. Res. Chin. Univ.*, 2021, **37**, 1158–1175.

154 R. Hinche, U. Khan, C. Falconi and S. W. Kim, *Mater. Today*, 2018, **21**, 611–630.

155 P. C. Sherrell, M. Fronzi, N. A. Shepelin, A. Corletto, D. A. Winkler, M. Ford, J. G. Shapter and A. V. Ellis, *Chem. Soc. Rev.*, 2022, **51**, 650–671.

156 J. C. Zhang, Q. Bai, X. L. Bi, C. H. Zhang, M. Y. Shi, W. W. Yu, F. L. Du, L. A. Wang, Z. B. Wang, Z. L. Zhu and N. Sui, *Nano Today*, 2022, **43**, 101429.

157 Y. Jia, Q. Jiang, H. Sun, P. Liu, D. Hu, Y. Pei, W. Liu, X. Crispin, S. Fabiano, Y. Ma and Y. Cao, *Adv. Mater.*, 2021, **33**, e2102990.

158 T. Q. Deng, X. Yong, W. Shi, Z. M. Wong, G. Wu, H. Pan, J. S. Wang and S. W. Yang, *J. Mater. Chem. A*, 2020, **8**, 4257–4262.

159 D. Li, Y. Gong, Y. Chen, J. Lin, Q. Khan, Y. Zhang, Y. Li, H. Zhang and H. Xie, *Nano-Micro Lett.*, 2020, **12**, 36.

160 P. H. Jiang, H. J. Liu, L. Cheng, D. D. Fan, J. Zhang, J. Wei, J. H. Liang and J. Shi, *Carbon*, 2017, **113**, 108–113.

161 P. F. Qi, K. Liu, S. P. Bi, Z. Chang, K. P. Yuan, Y. F. Gao, X. L. Zhang, Y. H. Jing and D. W. Tang, *ACS Appl. Energy Mater.*, 2022, **5**, 6363–6372.

162 L. Sun, P. H. Jiang, H. J. Liu, D. D. Fan, J. H. Liang, J. Wei, L. Cheng, J. Zhang and J. Shi, *Carbon*, 2015, **90**, 255–259.

163 S. M. Hatam-Lee, A. Rajabpour and S. Volz, *Carbon*, 2020, **161**, 816–826.

164 M. J. Wang, M. Z. Liao, L. H. Li, M. H. Li, Y. P. Chen, X. Hou, C. Yan, N. Jiang and J. H. Yu, *2D Mater.*, 2020, **7**, 035007.

165 L. Wang, B. Dong, R. Ge, F. Jiang and J. Xu, *ACS Appl. Mater. Interfaces*, 2017, **9**, 7108–7114.

166 Z. Xie, Y. Duo, Z. Lin, T. Fan, C. Xing, L. Yu, R. Wang, M. Qiu, Y. Zhang, Y. Zhao, X. Yan and H. Zhang, *Adv. Sci.*, 2020, **7**, 1902236.

167 Y. Nonoguchi, D. Sato and T. Kawai, *Polymers*, 2018, **10**, 962.

168 Z. Y. Hu, Z. H. Zhang, X. W. Cheng, F. C. Wang, Y. F. Zhang and S. L. Li, *Mater. Des.*, 2020, **191**, 108662.

169 Y. Liu, M. Calcabrini, Y. Yu, S. Lee, C. Chang, J. David, T. Ghosh, M. C. Spadaro, C. Xie, O. Cojocaru-Miredin, J. Arbiol and M. Ibanez, *ACS Nano*, 2022, **16**, 78–88.

170 X. Y. Zhou, Y. C. Yan, X. Lu, H. T. Zhu, X. D. Han, G. Chen and Z. F. Ren, *Mater. Today*, 2018, **21**, 974–988.

171 X. L. Shi, J. Zou and Z. G. Chen, *Chem. Rev.*, 2020, **120**, 7399–7515.

172 X. Bi, Q. Bai, L. Wang, F. Du, M. Liu, W. W. Yu, S. Li, J. Li, Z. Zhu, N. Sui and J. Zhang, *Nano Res.*, 2021, **15**, 1446–1454.

173 X. Fu, F. He, J. Gao, X. Yan, Q. Chang, Z. Zhang, C. Huang and Y. Li, *J. Am. Chem. Soc.*, 2023, **145**, 2759–2764.

174 X. Luan, L. Qi, Z. Zheng, Y. Gao, Y. Xue and Y. Li, *Angew. Chem., Int. Ed.*, 2023, **62**, e202215968.

175 F. Wang, J. An, H. Shen, Z. Wang, G. Li and Y. Li, *Angew. Chem., Int. Ed.*, 2023, **62**, e202216397.

176 T. Lu, X. Deng, Q. Sun, J. Xiao, J. He, K. Wang and C. Huang, *Small*, 2022, **18**, e2106328.

177 R. Dong, P. Han, H. Arora, M. Ballabio, M. Karakus, Z. Zhang, C. Shekhar, P. Adler, P. S. Petkov, A. Erbe, S. C. B. Mannsfeld, C. Felser, T. Heine, M. Bonn, X. Feng and E. Canovas, *Nat. Mater.*, 2018, **17**, 1027–1032.

178 J. Li, T. Jiu, S. Chen, L. Liu, Q. Yao, F. Bi, C. Zhao, Z. Wang, M. Zhao, G. Zhang, Y. Xue, F. Lu and Y. Li, *Nano Lett.*, 2018, **18**, 6941–6947.



179 L. Zhang, G. Ng, N. Kapoor-Kaushik, X. Shi, N. Corrigan, R. Webster, K. Jung and C. Boyer, *Angew. Chem., Int. Ed.*, 2021, **60**, 22664–22671.

180 W. Huang, W. Luo and Y. G. Li, *Mater. Today*, 2020, **40**, 160–172.

181 M. Majumder, M. S. Santosh, R. Viswanatha, A. K. Thakur, D. P. Dubal and K. Jayaramulu, *Energy Storage Mater.*, 2021, **37**, 396–416.

182 S. J. Kang, D. H. Lee, J. Kim, A. Capasso, H. S. Kang, J. W. Park, C. H. Lee and G. H. Lee, *2D Mater.*, 2020, **7**, 022003.

183 F. Wang, K. Pei, Y. Li, H. Li and T. Zhai, *Adv. Mater.*, 2021, **33**, e2005303.

184 T. Tan, X. Jiang, C. Wang, B. Yao and H. Zhang, *Adv. Sci.*, 2020, **7**, 2000058.

185 N. Rohaizad, C. C. Mayorga-Martinez, M. Fojtu, N. M. Latiff and M. Pumera, *Chem. Soc. Rev.*, 2021, **50**, 619–657.

186 C. Choi, Y. Lee, K. W. Cho, J. H. Koo and D. H. Kim, *Acc. Chem. Res.*, 2019, **52**, 73–81.

187 A. Bolotsky, D. Butler, C. Dong, K. Gerace, N. R. Glavin, C. Muratore, J. A. Robinson and A. Ebrahimi, *ACS Nano*, 2019, **13**, 9781–9810.

188 A. J. Ben-Sasson, J. L. Watson, W. Sheffler, M. C. Johnson, A. Bittleston, L. Somasundaram, J. Decarreau, F. Jiao, J. Chen, I. Mela, A. A. Drabek, S. M. Jarrett, S. C. Blacklow, C. F. Kaminski, G. L. Hura, J. J. De Yoreo, J. M. Kollman, H. Ruohola-Baker, E. Derivery and D. Baker, *Nature*, 2021, **589**, 468–473.

189 S. Kfir-Erenfeld, N. Haggiag, M. Biton, P. Stepensky, N. Assayag-Asherie and E. Yefenof, *Oncotarget*, 2017, **8**, 472–489.

190 J. X. Li, Q. W. Wang, H. Lu, Y. L. Han, L. L. Jiang, W. C. Qian, M. Zhu, B. N. Wang, J. S. Min, Y. Hou, S. N. Xu, Z. C. Xiong, H. B. Liu, Y. L. Li, C. Y. Chen, Y. Liu and P. X. Qian, *Nano Today*, 2022, **46**, 101622.

191 Q. Wang, Y. Liu, H. Wang, P. Jiang, W. Qian, M. You, Y. Han, X. Zeng, J. Li, H. Lu, L. Jiang, M. Zhu, S. Li, K. Huang, M. Tang, X. Wang, L. Yan, Z. Xiong, X. Shi, G. Bai, H. Liu, Y. Li, Y. Zhao, C. Chen and P. Qian, *Nat. Commun.*, 2022, **13**, 5657.

192 J. Liu, X. Shen, D. Baimanov, L. Wang, Y. Xiao, H. Liu, Y. Li, X. Gao, Y. Zhao and C. Chen, *ACS Appl. Mater. Interfaces*, 2019, **11**, 2647–2654.

